

$$\boxed{P_{\text{avg},x,T} = \frac{1}{T} \int_0^T |x(t)|^2 dt = \frac{T_0}{T} P_{\text{avg},x,T_0}} \quad (7B-14)$$

where

$$\boxed{P_{\text{avg},x,T_0} = \frac{1}{T_0} \int_0^{T_0} |x(t)|^2 dt = \frac{1}{T_0} \int_0^T |x(t)|^2 dt = \sum_{q=0}^{N+Z-1} |\hat{c}_q|^2} \quad (7B-15)$$

is the time-average power of $x(t)$ in the time interval $[0, T_0]$, $T_0 = (N+Z)T_s$ is the fundamental period of $x(t)$ in seconds, $T = NT_s$ is the duration of $x(t)$ in seconds, and \hat{c}_q is an estimate of the complex Fourier series coefficient c_q of $x(t)$ at harmonic q (frequency $f = qf_0$ Hz). Equation (7B-15) is Parseval's Relation from Fourier series theory. Note that $T \leq T_0$. If $x(t)$ has units of volts, then P_{avg,x,T_0} and $P_{\text{avg},x,T}$ have units of watts-ohms, and if $x(t)$ has units of amperes, then P_{avg,x,T_0} and $P_{\text{avg},x,T}$ have units of watts per ohm (see [Subsection 11.1.1](#)).

Power Spectrum

An estimate $\hat{S}_x(f)$ of the power spectrum $S_x(f)$ of $x(t)$ can be computed numerically as follows:

$$\boxed{\hat{S}_x(q) = \frac{1}{T} |\hat{X}(q)|^2, \quad q = 0, 1, \dots, N+Z-1} \quad (7B-16)$$

where

$$\hat{S}_x(q) \equiv \hat{S}_x(qf_0) = \hat{S}_x(f) \Big|_{f=qf_0}, \quad (7B-17)$$

$\hat{X}(q)$ is the numerical Fourier transform of $x(t)$ given by (7B-1), and T is the duration of $x(t)$ in seconds. If $x(t)$ has units of volts, then $\hat{S}_x(q)$ has units of $(W\cdot\Omega)/Hz$, and if $x(t)$ has units of amperes, then $\hat{S}_x(q)$ has units of $(W/\Omega)/Hz$.

Chapter 8

Array Theory – Planar Arrays

8.1 The Far-Field Beam Pattern of a Planar Array

Since a planar array is an example of a planar aperture, the far-field beam pattern (directivity function) of a planar array lying in the XY plane is given by the following two-dimensional spatial Fourier transform (see [Section 3.1](#)):

$$D(f, f_X, f_Y) = F_{x_A} F_{y_A} \{ A(f, x_A, y_A) \} \\ = \int_{-\infty}^{\infty} \int_{-\infty}^{\infty} A(f, x_A, y_A) \exp[+j2\pi(f_X x_A + f_Y y_A)] dx_A dy_A, \quad (8.1-1)$$

where $A(f, x_A, y_A)$ is the complex frequency response (complex aperture function) of the planar array, and

$$f_X = u/\lambda = \sin\theta \cos\psi/\lambda \quad (8.1-2)$$

and

$$f_Y = v/\lambda = \sin\theta \sin\psi/\lambda \quad (8.1-3)$$

are spatial frequencies in the X and Y directions, respectively, with units of cycles per meter. Since f_X and f_Y can be expressed in terms of the spherical angles θ and ψ , the far-field beam pattern can ultimately be expressed as a function of frequency f and the spherical angles θ and ψ , that is, $D(f, f_X, f_Y) \rightarrow D(f, \theta, \psi)$. We shall consider a field point to be in the far-field region of an array if the range r to the field point – as measured from the center of the array – satisfies the Fraunhofer (far-field) range criterion given by

$$r > \pi R_A^2 / \lambda > 2.414 R_A, \quad (8.1-4)$$

where R_A is the maximum radial extent of the array.

If a planar array lies in the XZ plane instead of the XY plane, then simply replace y_A and f_Y with z_A and f_Z , respectively, in (8.1-1), where spatial frequency f_Z is given by (1.2-45). And if a planar array lies in the YZ plane instead of the XY plane, then simply replace x_A and f_X with z_A and f_Z , respectively, in (8.1-1). As can be seen from (8.1-1), in order to derive the far-field beam pattern of a planar array, we must first specify a mathematical model for its complex frequency response.

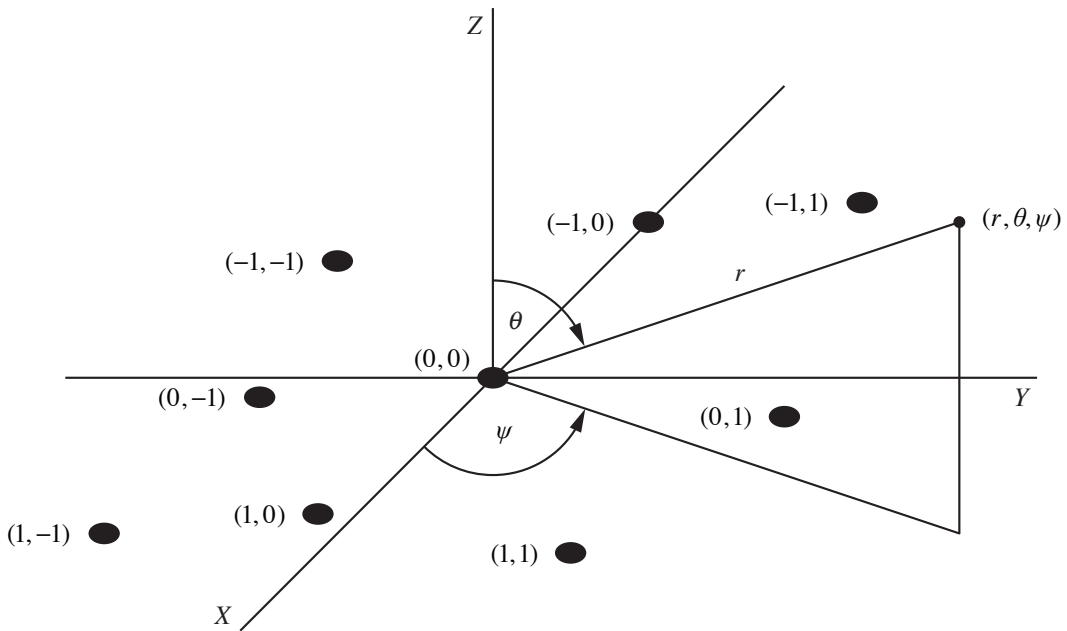


Figure 8.1-1 Planar array composed of an odd number of unevenly-spaced elements lying in the XY plane. Also shown are the element numbers (m,n) and a field point with spherical coordinates (r,θ,ψ) .

Consider a planar array composed of an *odd* number $M \times N$ of elements (electroacoustic transducers) lying in the XY plane, where M and N are the total odd number of elements in the X and Y directions, respectively (see Fig. 8.1-1). For example, the elements can be omnidirectional point-elements, rectangular pistons, or circular pistons. If the elements are *not* identical, that is, if each element has a different complex frequency response, and if the elements are *not* equally spaced, as shown in Fig. 8.1-1, then the complex frequency response (complex aperture function) of this array can be expressed as

$$A(f, x_A, y_A) = \sum_{m=-M'}^{M'} \sum_{n=-N'}^{N'} c_{mn}(f) e_{mn}(f, x_A - x_{mn}, y_A - y_{mn}), \quad (8.1-5)$$

where

$$M' = (M-1)/2, \quad (8.1-6)$$

$$N' = (N-1)/2, \quad (8.1-7)$$

$c_{mn}(f) = a_{mn}(f) \exp[+j\theta_{mn}(f)]$

(8.1-8)

is the frequency-dependent, *complex weight* associated with element (m, n) , $a_{mn}(f)$ is a real, frequency-dependent, *dimensionless*, amplitude weight, $\theta_{mn}(f)$ is a real, frequency-dependent, phase weight in radians, $e_{mn}(f, x_A, y_A)$ is the complex frequency response (complex aperture function) of element (m, n) , also known as the *element function*, and x_{mn} and y_{mn} are the x and y coordinates of the center of element (m, n) . Note that $x_{00}=0$ and $y_{00}=0$ because element $(0, 0)$ is centered at the origin of the coordinate system. Also note that, in general, $M \neq N$, and because the elements are not equally spaced, $x_{-m-n} \neq -x_{mn}$ and $y_{-m-n} \neq -y_{mn}$. Complex weights are implemented by using digital signal processing (digital beamforming) (see [Section 8.2](#)).

Equation (8.1-5) indicates that the complex frequency response of the array is modeled as the sum (superposition) of the complex-weighted frequency responses of all the elements in the array. The complex weights are used to control the complex frequency response of the array and, thus, the array's far-field beam pattern via amplitude and phase weighting. Substituting (8.1-5) into (8.1-1) yields the following expression for the far-field beam pattern:

$$D(f, f_X, f_Y) = \sum_{m=-M'}^{M'} \sum_{n=-N'}^{N'} c_{mn}(f) E_{mn}(f, f_X, f_Y) \exp[j2\pi(f_X x_{mn} + f_Y y_{mn})]$$

(8.1-9)

where

$$F_{x_A} F_{y_A} \{e_{mn}(f, x_A - x_{mn}, y_A - y_{mn})\} = E_{mn}(f, f_X, f_Y) \exp[j2\pi(f_X x_{mn} + f_Y y_{mn})]$$

(8.1-10)

and

$$E_{mn}(f, f_X, f_Y) = F_{x_A} F_{y_A} \{e_{mn}(f, x_A, y_A)\} \quad (8.1-11)$$

is the far-field beam pattern of element (electroacoustic transducer) (m, n) . The units of $e_{mn}(f, x_A, y_A)$, $A(f, x_A, y_A)$, $E_{mn}(f, f_X, f_Y)$, and $D(f, f_X, f_Y)$ are summarized in [Table 8.1-1](#).

If all the elements in the array are *identical* (i.e., all the elements have the same complex frequency response), but still *not* equally spaced, then (8.1-9) reduces to

$$D(f, f_X, f_Y) = E(f, f_X, f_Y) S(f, f_X, f_Y) \quad (8.1-12)$$

where

Table 8.1-1 Units of the Complex Frequency Responses $e_{mn}(f, x_A, y_A)$ and $A(f, x_A, y_A)$ and Corresponding Far-Field Beam Patterns $E_{mn}(f, f_X, f_Y)$ and $D(f, f_X, f_Y)$ for a Planar Array

Planar Array	$e_{mn}(f, x_A, y_A), A(f, x_A, y_A)$	$E_{mn}(f, f_X, f_Y), D(f, f_X, f_Y)$
active (transmit)	$\left(\left(m^3/\text{sec}\right)/V\right)/m^2$	$\left(m^3/\text{sec}\right)/V$
passive (receive)	$V/\left(m^2/\text{sec}\right)/m^2$	$V/\left(m^2/\text{sec}\right)$

$$E(f, f_X, f_Y) = F_{x_A} F_{y_A} \{e(f, x_A, y_A)\} \quad (8.1-13)$$

is the far-field beam pattern of *one* of the identical elements in the array,

$$S(f, f_X, f_Y) = \sum_{m=-M'}^{M'} \sum_{n=-N'}^{N'} c_{mn}(f) \exp[j2\pi(f_X x_{mn} + f_Y y_{mn})] \quad (8.1-14)$$

is the *array factor*, and if $a_{mn}(f) > 0 \ \forall m$ and n , then

$$S_{\max} = \max |S(f, f_X, f_Y)| = \sum_{m=-M'}^{M'} \sum_{n=-N'}^{N'} a_{mn}(f) \quad (8.1-15)$$

is the *normalization factor* for the array factor (see [Appendix 8B](#)). As can be seen from (8.1-14), $S(f, f_X, f_Y)$ is *dimensionless* and depends on the set of complex weights used and the locations (the x and y coordinates) of all the elements in the XY plane. The array factor $S(f, f_X, f_Y)$ contains the spatial information of the array. If one or more elements in the array are broken (not transmitting and/or receiving), set $c_{mn}(f) = 0$ for those elements. Equation (8.1-12) is referred to as the *Product Theorem* for a planar array composed of an odd number of identical elements. The Product Theorem states that the far-field beam pattern $D(f, f_X, f_Y)$ of a planar array composed of an odd number of *identical*, unevenly-spaced, complex-weighted elements is equal to the *product* of the far-field beam pattern $E(f, f_X, f_Y)$ of *one* of the identical elements in the array, and the dimensionless array factor $S(f, f_X, f_Y)$, which is related to the far-field beam pattern of an equivalent planar array composed of an odd number of identical, unevenly-spaced, complex-weighted, *omnidirectional point-elements*. Although the Product Theorem requires identical elements, equal spacing of the elements is *not* required. The interpretation of $S(f, f_X, f_Y)$ shall be discussed next.

Since an impulse function is used as a mathematical model for an omnidirectional point-source in acoustic wave propagation theory, the mathematical model that we shall use for the complex frequency response of an omnidirectional point-element lying in the XY plane is given by

$$e(f, x_A, y_A) = \mathcal{S}(f) \delta(x_A, y_A) = \mathcal{S}(f) \delta(x_A) \delta(y_A), \quad (8.1-16)$$

where $\mathcal{S}(f)$ is the complex, *element sensitivity function*. If the point-element is used in the active mode as a transmitter, then the element sensitivity function $\mathcal{S}(f)$ is referred to as the *transmitter sensitivity function* with units of $(m^3/sec)/V$ (see [Appendix 6B](#)). If the point-element is used in the passive mode as a receiver, then $\mathcal{S}(f)$ is referred to as the *receiver sensitivity function* with units of $V/(m^2/sec)$ (see [Appendix 6B](#)). Note that $\int_{-\infty}^{\infty} \int_{-\infty}^{\infty} e(f, x_A, y_A) dx_A dy_A = \mathcal{S}(f)$ because $\int_{-\infty}^{\infty} \delta(x_A) dx_A \int_{-\infty}^{\infty} \delta(y_A) dy_A = 1$. The impulse function $\delta(x_A, y_A) = \delta(x_A) \delta(y_A)$ has units of inverse squared-meters (m^{-2}). The units of $\mathcal{S}(f)$ are summarized in [Table 8.1-2](#).

Table 8.1-2 Units of the Element Sensitivity Function $\mathcal{S}(f)$

Omnidirectional Point-Element	$\mathcal{S}(f)$
active (transmit)	$(m^3/sec)/V$
passive (receive)	$V/(m^2/sec)$

Since

$$F_{x_A} F_{y_A} \{ \delta(x_A, y_A) \} = F_{x_A} \{ \delta(x_A) \} F_{y_A} \{ \delta(y_A) \} = 1, \quad (8.1-17)$$

taking the two-dimensional spatial Fourier transform of (8.1-16) yields

$$E(f, f_X, f_Y) = \mathcal{S}(f). \quad (8.1-18)$$

Equation (8.1-18) is the far-field beam pattern of an omnidirectional point-element and as expected, it is *not* a function of the spherical angles θ and ψ . The term “omnidirectional” means that an electroacoustic transducer transmits and/or receives equally well in all directions. Therefore, by substituting (8.1-18) into (8.1-12), we obtain the following expression for the far-field beam pattern of a

planar array composed of an odd number $M \times N$ of identical, unevenly-spaced, complex-weighted, *omnidirectional point-elements* lying in the XY plane, where M and N are the total odd number of elements in the X and Y directions, respectively:

$$D(f, f_X, f_Y) = \mathcal{S}(f) S(f, f_X, f_Y) \quad (8.1-19)$$

where $S(f, f_X, f_Y)$ is given by (8.1-14). The corresponding complex frequency response (complex aperture function) of the array can be obtained by taking the inverse two-dimensional spatial Fourier transform of (8.1-19). Doing so yields

$$A(f, x_A, y_A) = \mathcal{S}(f) \sum_{m=-M'}^{M'} \sum_{n=-N'}^{N'} c_{mn}(f) \delta(x_A - x_{mn}) \delta(y_A - y_{mn}) \quad (8.1-20)$$

since

$$\begin{aligned} F_{f_X}^{-1} F_{f_Y}^{-1} \left\{ \exp \left[+j2\pi(f_X x_{mn} + f_Y y_{mn}) \right] \right\} &= F_{f_X}^{-1} \left\{ \exp(+j2\pi f_X x_{mn}) \right\} F_{f_Y}^{-1} \left\{ \exp(+j2\pi f_Y y_{mn}) \right\} \\ &= \delta(x_A - x_{mn}) \delta(y_A - y_{mn}). \end{aligned} \quad (8.1-21)$$

Note that the double summation in (8.1-20) is in the form of the impulse response of a two-dimensional, finite impulse response (FIR) digital filter. In [Appendix 8A](#), it is shown that a planar array composed of an odd number of identical, complex-weighted elements can be thought of as a two-dimensional, spatial FIR filter, where $s(f, x_A, y_A) = F_{f_X}^{-1} F_{f_Y}^{-1} \{ S(f, f_X, f_Y) \}$ is the spatial impulse response of the array at frequency f hertz.

Finally, if all the elements in the array are *equally spaced* in the X direction, and *equally spaced* in the Y direction, then

$$x_{mn} = x_m = m d_X, \quad m = -M', \dots, 0, \dots, M' \quad (8.1-22)$$

and

$$y_{mn} = y_n = n d_Y, \quad n = -N', \dots, 0, \dots, N' \quad (8.1-23)$$

where d_X and d_Y are the *interelement spacings* in meters in the X and Y directions, respectively. Note that, in general, $d_X \neq d_Y$.

Example 8.1-1 Planar Array of Rectangular Pistons

Consider a planar array composed of an odd number $M \times N$ of identical,

unevenly-spaced, complex-weighted, rectangular pistons lying in the XY plane, where M and N are the total odd number of elements in the X and Y directions, respectively. Since the elements are identical, the Product Theorem given by (8.1-12) shall be used to obtain the far-field beam pattern of the array. The element function is given by (see [Section 3.2](#))

$$e(f, x_A, y_A) = A_A \operatorname{rect}(x_A/L_X) \operatorname{rect}(y_A/L_Y), \quad (8.1-24)$$

with corresponding unnormalized, far-field beam pattern

$$E(f, f_X, f_Y) = A_A L_X L_Y \operatorname{sinc}(f_X L_X) \operatorname{sinc}(f_Y L_Y), \quad (8.1-25)$$

where the real, positive constant A_A carries the correct units of $e(f, x_A, y_A)$ (see [Table 8.1-1](#)), and $L_X L_Y$ is the area of an individual rectangular piston in squared meters. Although A_A is shown here as a constant, as was previously mentioned in [Section 3.2](#), A_A is, in general, a real, nonnegative function of frequency, that is, $A_A \rightarrow A_A(f)$. Therefore, substituting (8.1-25) into (8.1-12) yields the following expression for the unnormalized, far-field beam pattern of the array:

$$D(f, f_X, f_Y) = A_A L_X L_Y \operatorname{sinc}(f_X L_X) \operatorname{sinc}(f_Y L_Y) S(f, f_X, f_Y), \quad (8.1-26)$$

where $S(f, f_X, f_Y)$ is given by (8.1-14). If all the elements in the array are equally spaced in the X direction, and equally spaced in the Y direction, then substitute (8.1-22) and (8.1-23) into (8.1-14).

If L_X and L_Y are small compared to a wavelength so that

$$L_X/\lambda \leq 0.0278 \quad (8.1-27)$$

and

$$L_Y/\lambda \leq 0.0278, \quad (8.1-28)$$

then (8.1-25) reduces to (see [Example 6.2-1](#))

$$E(f, f_X, f_Y) \approx A_A L_X L_Y, \quad L_X/\lambda \leq 0.0278, \quad L_Y/\lambda \leq 0.0278. \quad (8.1-29)$$

Therefore, the rectangular pistons act like omnidirectional point-elements because the far-field beam pattern $E(f, f_X, f_Y)$ is not a function of the spherical angles θ and ψ . Substituting (8.1-29) into (8.1-12) yields the following expression for the unnormalized, far-field beam pattern of the array:

$$D(f, f_X, f_Y) \approx A_A L_X L_Y S(f, f_X, f_Y), \quad L_X/\lambda \leq 0.0278, \quad L_Y/\lambda \leq 0.0278. \quad (8.1-30)$$

Compare (8.1-30) with (8.1-26) and (8.1-19). If we let $L_{\max} = 0.0278\lambda$, then the far-field beam patterns $E(f, f_X, f_Y)$ and $D(f, f_X, f_Y)$ given by (8.1-29) and (8.1-30) are valid as long as $L_X \leq L_{\max}$ and $L_Y \leq L_{\max}$ (see [Table 8.1-3](#)). ■

Table 8.1-3 Values for the Maximum Length $L_{\max} = 0.0278\lambda$ for Three Different Frequencies f . Note that 1 in = 2.54 cm .

c (m/sec)	f (kHz)	λ (m)	L_{\max} (cm)	L_{\max} (in)
1500	0.1	15.0	41.7	16.4
1500	1.0	1.5	4.17	1.64
1500	10.0	0.15	0.417	0.164

Example 8.1-2 Planar Array of Circular Pistons

Consider a planar array composed of an odd number $M \times N$ of identical, unevenly-spaced, complex-weighted, circular pistons lying in the XY plane, where M and N are the total odd number of elements in the X and Y directions, respectively. Since the elements are identical, the Product Theorem given by (8.1-12) shall be used to obtain the far-field beam pattern of the array. From [Section 3.3](#), the element function is given by

$$e(f, r_A, \phi_A) = A_A \text{circ}(r_A/a), \quad (8.1-31)$$

with corresponding unnormalized, far-field beam pattern

$$E(f, \theta, \psi) = 2A_A \pi a^2 \frac{J_1\left(\frac{2\pi a}{\lambda} \sin \theta\right)}{\frac{2\pi a}{\lambda} \sin \theta}, \quad (8.1-32)$$

where the real, positive constant A_A carries the correct units of $e(f, r_A, \phi_A)$ (see [Table 8.1-1](#)), a is the radius of an individual circular piston in meters, and πa^2 is the area of an individual circular piston in squared meters. Although A_A is shown here as a constant, as was previously mentioned in [Section 3.3](#), A_A is, in general, a real, nonnegative function of frequency, that is, $A_A \rightarrow A_A(f)$. Therefore, substituting (8.1-32) into (8.1-12) yields the following expression for the unnormalized, far-field beam pattern of the array:

$$D(f, \theta, \psi) = 2A_A \pi a^2 \frac{J_1\left(\frac{2\pi a}{\lambda} \sin \theta\right)}{\frac{2\pi a}{\lambda} \sin \theta} S(f, \theta, \psi), \quad (8.1-33)$$

where $S(f, \theta, \psi)$ is obtained by substituting f_x and f_y given by (8.1-2) and (8.1-3), respectively, into (8.1-14). If all the elements in the array are equally spaced in the X direction, and equally spaced in the Y direction, then substitute (8.1-22) and (8.1-23) into (8.1-14).

If the circumference $2\pi a$ of a circular piston is small compared to a wavelength so that

$$2\pi a/\lambda < 1, \quad (8.1-34)$$

then the magnitude of the argument of the Bessel function will also be less than 1 because $|\sin \theta| \leq 1$. Since

$$J_1(x) = \frac{x}{2} - \frac{2x^3}{2 \times 4^2} + \frac{3x^5}{2 \times 4^2 \times 6^2} - \dots, \quad (8.1-35)$$

by using only the first term in the series expansion given by (8.1-35),

$$J_1\left(\frac{2\pi a}{\lambda} \sin \theta\right) \approx \frac{\pi a}{\lambda} \sin \theta, \quad \frac{2\pi a}{\lambda} < 1. \quad (8.1-36)$$

Substituting (8.1-36) into (8.1-32) yields

$$E(f, \theta, \psi) \approx A_A \pi a^2, \quad 2\pi a/\lambda < 1. \quad (8.1-37)$$

Therefore, the circular pistons act like omnidirectional point-elements because the far-field beam pattern $E(f, \theta, \psi)$ is not a function of the spherical angles θ and ψ . Substituting (8.1-37) into (8.1-12) yields the following expression for the unnormalized, far-field beam pattern of the array:

$$D(f, \theta, \psi) \approx A_A \pi a^2 S(f, \theta, \psi), \quad 2\pi a/\lambda < 1, \quad (8.1-38)$$

or

$$D(f, f_x, f_y) \approx A_A \pi a^2 S(f, f_x, f_y), \quad 2\pi a/\lambda < 1, \quad (8.1-39)$$

where $S(f, f_x, f_y)$ is given by (8.1-14). Compare (8.1-38) with (8.1-33), and compare (8.1-39) with (8.1-19). If we let $a_{\max} = \lambda/(2\pi)$, then the far-field beam patterns $E(f, \theta, \psi)$ and $D(f, \theta, \psi)$ given by (8.1-37) and (8.1-38) are valid as long as $a < a_{\max}$ (see Table 8.1-4). By comparing Tables 8.1-3 and 8.1-4, it can be

seen that for the same value of frequency, a circular piston with a bigger area than a rectangular piston can still act like an omnidirectional point-element. In other words, it is easier for a circular piston to act like an omnidirectional point-element than a rectangular piston. ■

Table 8.1-4 Values for the Maximum Radius $a_{\max} = \lambda/(2\pi)$ for Three Different Frequencies f . Note that 1 in = 2.54 cm .

c (m/sec)	f (kHz)	λ (m)	a_{\max} (cm)	a_{\max} (in)
1500	0.1	15.0	238.7	94.0
1500	1.0	1.5	23.87	9.4
1500	10.0	0.15	2.387	0.94

Example 8.1-3 Separable Complex Weights

The product theorem for planar arrays given by (8.1-12) is a general expression. A somewhat simplified version of (8.1-12) can be obtained if the identical elements are *equally spaced* in the X direction, and *equally spaced* in the Y direction, and the complex weights $c_{mn}(f)$ are *separable*. If the complex weights are separable, then

$$c_{mn}(f) = c_m(f)w_n(f), \quad (8.1-40)$$

where

$$c_m(f) = a_m(f)\exp[+j\theta_m(f)] \quad (8.1-41)$$

is a frequency-dependent, complex weight in the X direction, and

$$w_n(f) = b_n(f)\exp[+j\phi_n(f)] \quad (8.1-42)$$

is a frequency-dependent, complex weight in the Y direction, where $a_m(f)$ and $b_n(f)$ are real, frequency-dependent, dimensionless, amplitude weights, and $\theta_m(f)$ and $\phi_n(f)$ are real, frequency-dependent, phase weights in radians. Equation (8.1-40) indicates that the set of complex weights in the X direction is independent of the set of complex weights in the Y direction.

Therefore, substituting (8.1-22), (8.1-23), and (8.1-40) into (8.1-14) yields

$S(f, f_X, f_Y) = S_X(f, f_X)S_Y(f, f_Y)$

(8.1-43)

where

$$S_X(f, f_X) = \sum_{m=-M'}^{M'} c_m(f) \exp(+j2\pi f_X m d_X) \quad (8.1-44)$$

and

$$S_Y(f, f_Y) = \sum_{n=-N'}^{N'} w_n(f) \exp(+j2\pi f_Y n d_Y) \quad (8.1-45)$$

and by substituting (8.1-43) into (8.1-12), we obtain the following version of the Product Theorem:

$$D(f, f_X, f_Y) = E(f, f_X, f_Y) S_X(f, f_X) S_Y(f, f_Y) \quad (8.1-46)$$

■

Example 8.1-4 Tesserel Quadrupole

Consider a planar array of four identical, complex-weighted, omnidirectional point-elements lying in the XY plane as shown in Fig. 8.1-2. Let the interelement spacings in both the X and Y directions be equal to d meters, that is, $d_Y = d_X = d$. The planar array shown in Fig. 8.1-2 with $d_Y = d_X = d$, and the amplitude and phase weights given in Table 8.1-5 is known as a *tesserel quadrupole*.

Table 8.1-5 The x and y Coordinates of the Centers of the Elements, and the Associated Amplitude and Phase Weights of a Tesserel Quadrupole Lying in the XY Plane

(m, n)	x_{mn}	y_{mn}	$a_{mn}(f)$	$\theta_{mn}(f)$
$(-1, -1)$	$-d/2$	$-d/2$	$a(f)$	$-\theta_{11}(f)$
$(-1, 1)$	$-d/2$	$d/2$	$-a(f)$	$-\theta_{1-1}(f)$
$(1, -1)$	$d/2$	$-d/2$	$-a(f)$	$\theta_{1-1}(f)$
$(1, 1)$	$d/2$	$d/2$	$a(f)$	$\theta_{11}(f)$

In order to derive the far-field beam pattern of the tesserel quadrupole, we shall first model its complex frequency response. By using the mathematical model for the complex frequency response of an omnidirectional point-element as given by (8.1-16) and the principle of superposition, the complex frequency

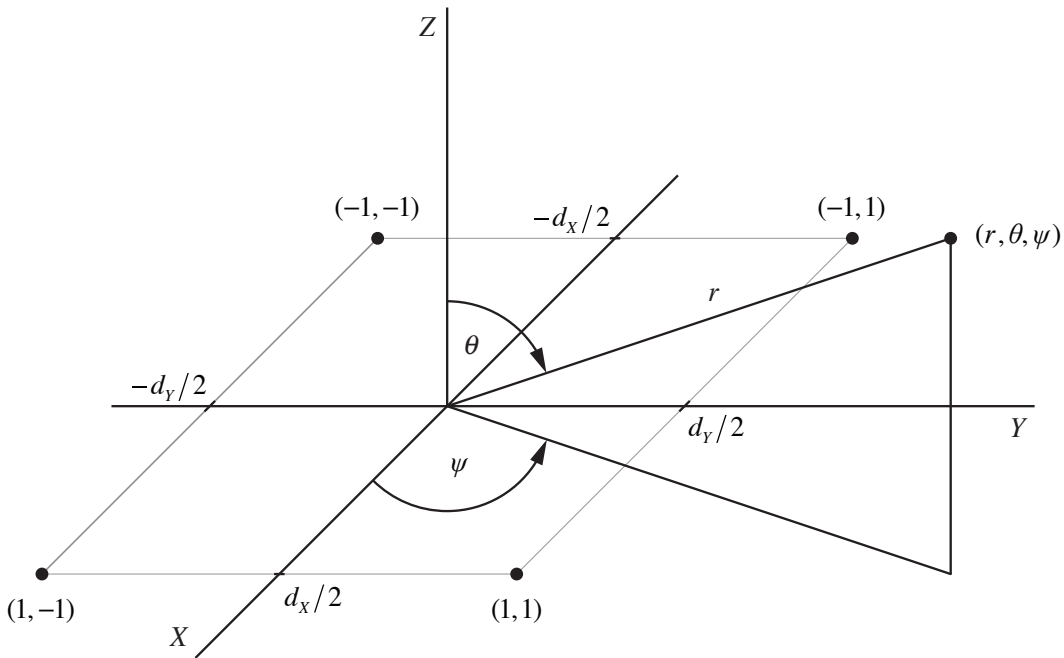


Figure 8.1-2 Planar array of four identical, omnidirectional point-elements lying in the XY plane. Also shown are the element numbers (m, n) and a field point with spherical coordinates (r, θ, ψ) .

response (complex aperture function) of the tesseral quadrupole can be expressed as the sum of the complex-weighted frequency responses of all the elements in the array as follows:

$$\begin{aligned}
 A(f, x_A, y_A) = & c_{-1-1}(f) \mathcal{S}(f) \delta(x_A - x_{-1-1}) \delta(y_A - y_{-1-1}) + \\
 & c_{-11}(f) \mathcal{S}(f) \delta(x_A - x_{-11}) \delta(y_A - y_{-11}) + \\
 & c_{1-1}(f) \mathcal{S}(f) \delta(x_A - x_{1-1}) \delta(y_A - y_{1-1}) + \\
 & c_{11}(f) \mathcal{S}(f) \delta(x_A - x_{11}) \delta(y_A - y_{11}),
 \end{aligned} \tag{8.1-47}$$

where $\mathcal{S}(f)$ is the complex, element sensitivity function. Since [see (8.1-21)]

$$\begin{aligned}
 F_{x_A} F_{y_A} \left\{ \delta(x_A - x_{mn}) \delta(y_A - y_{mn}) \right\} &= F_{x_A} \left\{ \delta(x_A - x_{mn}) \right\} F_{y_A} \left\{ \delta(y_A - y_{mn}) \right\} \\
 &= \exp \left[+j2\pi(f_X x_{mn} + f_Y y_{mn}) \right],
 \end{aligned} \tag{8.1-48}$$

taking the two-dimensional spatial Fourier transform of (8.1-47) with respect to x_A and y_A yields

$$\begin{aligned}
D(f, f_X, f_Y) = & c_{-1-1}(f) \mathcal{S}(f) \exp[j2\pi(f_X x_{-1-1} + f_Y y_{-1-1})] + \\
& c_{-11}(f) \mathcal{S}(f) \exp[j2\pi(f_X x_{-11} + f_Y y_{-11})] + \\
& c_{1-1}(f) \mathcal{S}(f) \exp[j2\pi(f_X x_{1-1} + f_Y y_{1-1})] + \\
& c_{11}(f) \mathcal{S}(f) \exp[j2\pi(f_X x_{11} + f_Y y_{11})].
\end{aligned} \tag{8.1-49}$$

Substituting (8.1-8) and the specifications given in [Table 8.1-5](#) into (8.1-49) and rearranging terms yields

$$\begin{aligned}
D(f, f_X, f_Y) = & a(f) \mathcal{S}(f) \times \\
& \left\{ \left[\exp\left\{ j[\pi(f_X + f_Y)d + \theta_{11}(f)] \right\} + \exp\left\{ -j[\pi(f_X + f_Y)d + \theta_{11}(f)] \right\} \right] - \right. \\
& \left. \left[\exp\left\{ j[\pi(f_X - f_Y)d + \theta_{1-1}(f)] \right\} + \exp\left\{ -j[\pi(f_X - f_Y)d + \theta_{1-1}(f)] \right\} \right] \right\},
\end{aligned} \tag{8.1-50}$$

or

$$\begin{aligned}
D(f, f_X, f_Y) = & 2a(f) \mathcal{S}(f) \times \\
& \left\{ \cos[\pi(f_X + f_Y)d + \theta_{11}(f)] - \cos[\pi(f_X - f_Y)d + \theta_{1-1}(f)] \right\}.
\end{aligned} \tag{8.1-51}$$

Because we have not yet discussed phase weights for planar arrays in any great detail, let $\theta_{11}(f) = 0$ and $\theta_{1-1}(f) = 0$. In other words, if only amplitude weighting is done (no phase weighting), then (8.1-51) reduces to

$$D(f, f_X, f_Y) = 2a(f) \mathcal{S}(f) [\cos(\pi f_X d + \pi f_Y d) - \cos(\pi f_X d - \pi f_Y d)], \tag{8.1-52}$$

and by using the trigonometric identity

$$\cos(\alpha + \beta) - \cos(\alpha - \beta) = -2 \sin \alpha \sin \beta, \tag{8.1-53}$$

(8.1-52) can be rewritten as

$$D(f, f_X, f_Y) = -4a(f) \mathcal{S}(f) \sin(\pi f_X d) \sin(\pi f_Y d)$$

(8.1-54)

where $\mathcal{S}(f)$ is the complex, element sensitivity function. Equation (8.1-54) is the *unnormalized*, far-field beam pattern of a tesseral quadrupole lying in the XY

plane with no phase weighting.

The magnitude of the far-field beam pattern given by (8.1-54) is

$$|D(f, f_X, f_Y)| = 4 |a(f)| |\mathcal{S}(f)| |\sin(\pi f_X d)| |\sin(\pi f_Y d)|, \quad (8.1-55)$$

and since the maximum value of the magnitude of a sine function is 1, the normalization factor is

$$D_{\max} = \max |D(f, f_X, f_Y)| = 4 |a(f)| |\mathcal{S}(f)|. \quad (8.1-56)$$

Dividing (8.1-55) by (8.1-56) yields the following expression for the magnitude of the *normalized*, far-field beam pattern of a tesseral quadrupole lying in the *XY* plane with no phase weighting:

$$|D_N(f, f_X, f_Y)| = |\sin(\pi f_X d)| |\sin(\pi f_Y d)| \quad (8.1-57)$$

Since spatial frequencies

$$f_X = u/\lambda = \sin \theta \cos \psi / \lambda \quad (8.1-58)$$

and

$$f_Y = v/\lambda = \sin \theta \sin \psi / \lambda, \quad (8.1-59)$$

(8.1-57) can also be expressed as

$$|D_N(f, u, v)| = \left| \sin\left(\pi \frac{d}{\lambda} u\right) \right| \left| \sin\left(\pi \frac{d}{\lambda} v\right) \right|, \quad (8.1-60)$$

or

$$|D_N(f, \theta, \psi)| = \left| \sin\left(\pi \frac{d}{\lambda} \sin \theta \cos \psi\right) \right| \left| \sin\left(\pi \frac{d}{\lambda} \sin \theta \sin \psi\right) \right|. \quad (8.1-61)$$

At broadside ($\theta = 0^\circ$) where direction cosines $u = 0$ and $v = 0$, (8.1-60) and (8.1-61) reduce to $|D_N(f, 0, 0)| = 0$ and $|D_N(f, 0^\circ, \psi)| = 0$, respectively. Furthermore, in the *XZ* plane where $\psi = 0^\circ$ or $\psi = 180^\circ$, $v = 0$. As a result, (8.1-60) reduces to $|D_N(f, u, 0)| = 0$, and (8.1-61) reduces to $|D_N(f, \theta, 0^\circ)| = 0$ and $|D_N(f, \theta, 180^\circ)| = 0$. Similarly, in the *YZ* plane where $\psi = 90^\circ$ or $\psi = 270^\circ$, $u = 0$. As a result, (8.1-60) reduces to $|D_N(f, 0, v)| = 0$ and (8.1-61) reduces to $|D_N(f, \theta, 90^\circ)| = 0$ and $|D_N(f, \theta, 270^\circ)| = 0$. Therefore, the far-field beam pattern of the tesseral quadrupole not only has a null at broadside like the far-field beam patterns of both the dipole (see Fig. 6.1-4) and the axial quadrupole (see Fig. 6.1-9), it also has nulls in the *XZ* and *YZ* planes. And finally, if $d/\lambda = 0.5$, then

$|D_N(f, u, v)| = 1$ when $(u, v) = (-1, -1), (-1, 1), (1, -1)$, and $(1, 1)$. However, these (u, v) coordinates do not lie inside or on the unit circle (see Fig. 8.1-3). ■

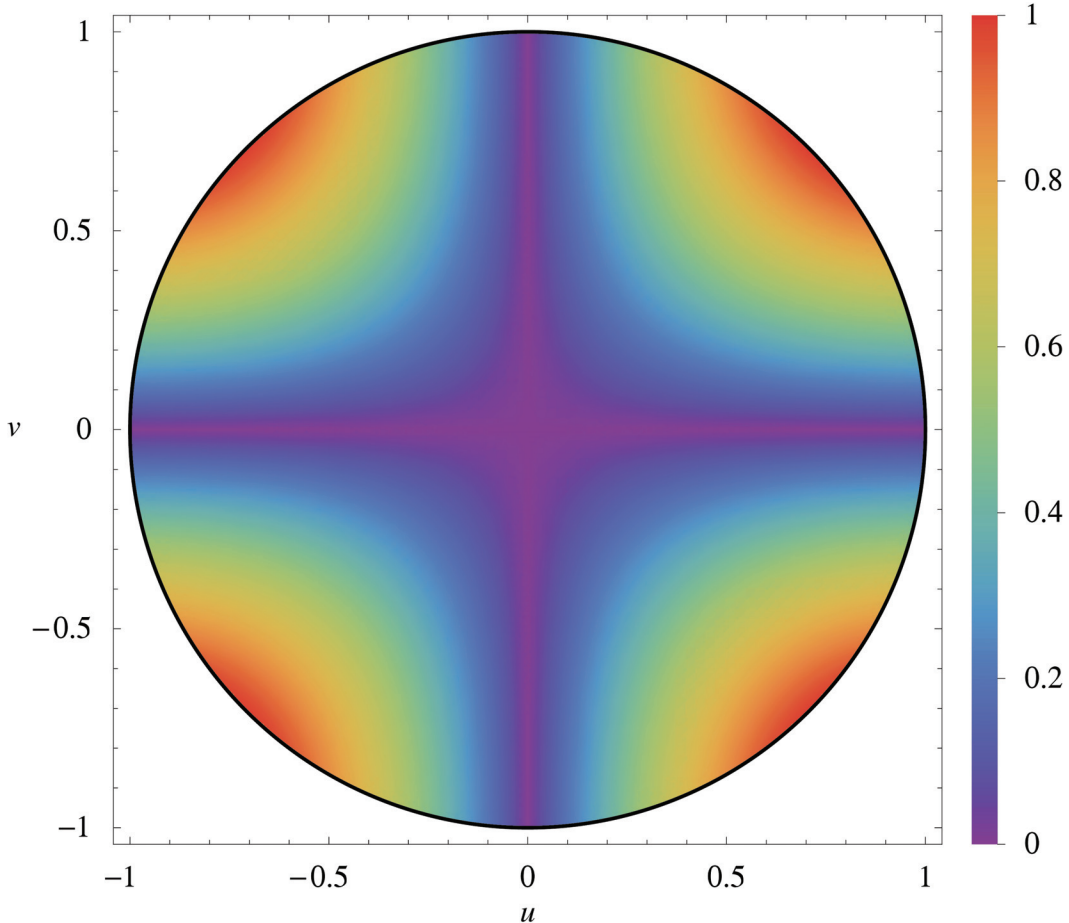


Figure 8.1-3 Magnitude of the normalized, far-field beam pattern of a tesseral quadrupole lying in the XY plane, plotted as a function of direction cosines u and v for $d/\lambda = 0.5$.

Example 8.1-5 Main Lobe in a Half-Space

Consider a planar array of four identical, complex-weighted, omnidirectional point-elements lying in the XY plane as shown in Fig. 8.1-2. The elements are equally spaced in the X direction, and equally spaced in the Y direction. If the complex weights $c_{mn}(f)$ are separable [see (8.1-40)], and since $E(f, f_X, f_Y) = \mathcal{S}(f)$, where $\mathcal{S}(f)$ is the complex, element sensitivity function, then the unnormalized, far-field beam pattern of this array is given by the Product

Theorem [see (8.1-46)]

$$D(f, f_X, f_Y) = \mathcal{S}(f) S_X(f, f_X) S_Y(f, f_Y), \quad (8.1-62)$$

where

$$S_X(f, f_X) = c_{-1}(f) \exp(+j2\pi f_X x_{-1}) + c_1(f) \exp(+j2\pi f_X x_1) \quad (8.1-63)$$

and

$$S_Y(f, f_Y) = w_{-1}(f) \exp(+j2\pi f_Y y_{-1}) + w_1(f) \exp(+j2\pi f_Y y_1) \quad (8.1-64)$$

since there are two elements in both the X and Y directions [see (6.1-12)]. The x and y coordinates of the centers of the elements, and the associated complex weights are given in [Table 8.1-6](#).

Table 8.1-6 The x and y Coordinates of the Centers of the Elements, and the Associated Complex Weights of a Four-Element Planar Array Lying in the XY Plane

x_1	x_{-1}	$c_1(f)$	$c_{-1}(f)$	y_1	y_{-1}	$w_1(f)$	$w_{-1}(f)$
$d_x/2$	$-d_x/2$	$a(f)$	$a(f) \exp(\pm j\pi/2)$	$d_y/2$	$-d_y/2$	$b(f)$	$b(f)$

Substituting the specifications given in [Table 8.1-6](#) into (8.1-63) and (8.1-64) yields

$$S_X(f, f_X) = 2a(f) \cos[\pi f_X d_X \mp (\pi/4)] \exp(\pm j\pi/4) \quad (8.1-65)$$

and

$$S_Y(f, f_Y) = 2b(f) \cos(\pi f_Y d_Y), \quad (8.1-66)$$

respectively, and by substituting (8.1-65) and (8.1-66) into (8.1-62), we obtain

$$D(f, f_X, f_Y) = 4a(f)b(f)\mathcal{S}(f) \cos[\pi f_X d_X \mp (\pi/4)] \cos(\pi f_Y d_Y) \exp(\pm j\pi/4). \quad (8.1-67)$$

If the interelement spacings

$$d_X = \lambda/4 \quad (8.1-68)$$

and

$$d_Y = \lambda/2, \quad (8.1-69)$$

and by using (8.1-58) and (8.1-59), (8.1-67) can be rewritten as

$$D(f, u, v) = 4 |a(f)| |b(f)| |\mathcal{S}(f)| \cos[\pi(u \mp 1)/4] \cos(\pi v/2) \exp(\pm j\pi/4)$$

(8.1-70)

Equation (8.1-70) is the *unnormalized*, far-field beam pattern of the array with interelement spacings given by (8.1-68) and (8.1-69), where $\mathcal{S}(f)$ is the complex element sensitivity function.

The magnitude of the far-field beam pattern given by (8.1-70) is

$$|D(f, u, v)| = 4 |a(f)| |b(f)| |\mathcal{S}(f)| |\cos[\pi(u \mp 1)/4]| |\cos(\pi v/2)|, \quad (8.1-71)$$

and since the maximum value of $|\cos[\pi(u \mp 1)/4]| |\cos(\pi v/2)|$ occurs at $u = \pm 1$ and $v = 0$ where $|\cos(0)| |\cos(0)| = 1$, the normalization factor is

$$D_{\max} = \max |D(f, u, v)| = 4 |a(f)| |b(f)| |\mathcal{S}(f)|. \quad (8.1-72)$$

Note that $u = \pm 1$ are the end-fire locations in direction-cosine space in the X direction. Dividing (8.1-71) by (8.1-72) yields the following expression for the magnitude of the *normalized*, far-field beam pattern of the array:

$$|D_N(f, u, v)| = |\cos[\pi(u \mp 1)/4]| |\cos(\pi v/2)| \quad (8.1-73)$$

where $|D_N(f, \pm 1, 0)| = 1$. Substituting $u = \sin \theta \cos \psi$ and $v = \sin \theta \sin \psi$ into (8.1-73) yields

$$|D_N(f, \theta, \psi)| = \left| \cos \left[\frac{\pi}{4} (\sin \theta \cos \psi \mp 1) \right] \right| \left| \cos \left(\frac{\pi}{2} \sin \theta \sin \psi \right) \right|, \quad (8.1-74)$$

and by setting $\theta = 90^\circ$ in (8.1-74), we obtain

$$|D_N(f, 90^\circ, \psi)| = \left| \cos \left[\frac{\pi}{4} (\cos \psi \mp 1) \right] \right| \left| \cos \left(\frac{\pi}{2} \sin \psi \right) \right|, \quad (8.1-75)$$

which is the magnitude of the normalized, *horizontal*, far-field beam pattern in the XY plane. The \mp sign on the right-hand side of (8.1-75) corresponds to the $\pm \pi/2$ phase weight in Table 8.1-6 (see Figs. 8.1-4 and 8.1-5). Like the cardioid beam patterns in Example 6.1-3, the main lobes of the beam patterns in Figs. 8.1-4 and 8.1-5 exist in a half-space. A *twin-line planar array*, which is one solution to the port/starboard (left/right) ambiguity problem associated with linear arrays, and is a generalization of the planar array shown in Fig. 8.1-2, is discussed in Example 8.2-1. ■

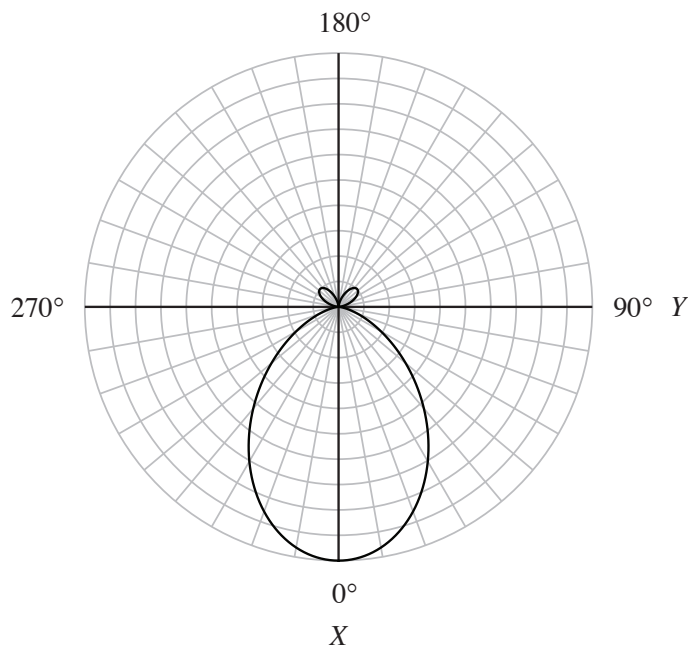


Figure 8.1-4 Polar plot, as a function of the azimuthal (bearing) angle ψ , of the magnitude of the normalized, horizontal, far-field beam pattern given by (8.1-75) for the phase weight $\pi/2$ in [Table 8.1-6](#).

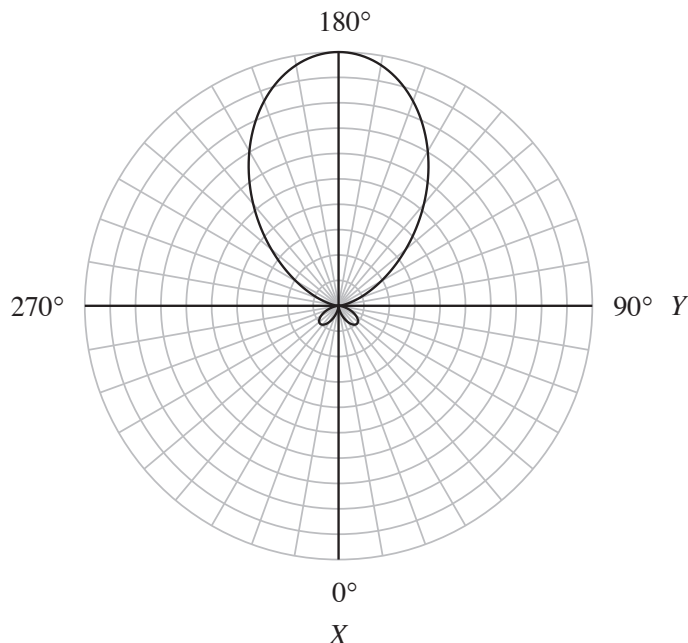


Figure 8.1-5 Polar plot, as a function of the azimuthal (bearing) angle ψ , of the magnitude of the normalized, horizontal, far-field beam pattern given by (8.1-75) for the phase weight $-\pi/2$ in [Table 8.1-6](#).

Example 8.1-6 Concentric Circular Arrays

In [Section 3.3](#) it was shown that the far-field beam pattern of a planar, circular aperture lying in the XY plane with radius a meters and with complex frequency response (complex aperture function) expressed in terms of the polar coordinates r_A and ϕ_A is given by (see [Figures 3.3-1](#) and [3.3-2](#))

$$D(f, \theta, \psi) = \int_0^{2\pi} \int_0^a A(f, r_A, \phi_A) \exp\left[j \frac{2\pi r_A}{\lambda} \sin \theta \cos(\psi - \phi_A)\right] r_A dr_A d\phi_A. \quad (8.1-76)$$

In this example we shall use (8.1-76) to derive the far-field beam pattern of a planar array of *concentric circular arrays* of identical, equally-spaced, complex-weighted, omnidirectional point-elements lying in the XY plane (see [Fig. 8.1-6](#)). However, in order to use (8.1-76), we first need to model the complex frequency response $A(f, r_A, \phi_A)$ of the planar array.

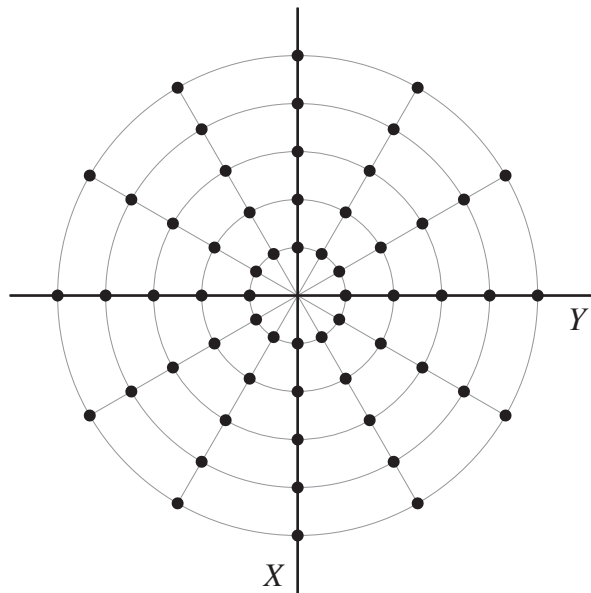


Figure 8.1-6 Planar array of concentric circular arrays of identical, equally-spaced, omnidirectional point-elements lying in the XY plane.

The mathematical model for the complex frequency response of an omnidirectional point-element can be expressed in polar coordinates as

$$e(f, r_A - r_0, \phi_A - \phi_0) = \mathcal{S}(f) \frac{\delta(r_A - r_0)}{r_A} \delta(\phi_A - \phi_0), \quad (8.1-77)$$

where $\mathcal{S}(f)$ is the complex, element sensitivity function, and (r_0, ϕ_0) are the polar coordinates of the center of the element. Note that $\int_0^{2\pi} \int_0^{\infty} e(f, r_A - r_0, \phi_A - \phi_0) r_A dr_A d\phi_A = \mathcal{S}(f)$ because $\int_0^{\infty} \delta(r_A - r_0) dr_A \int_0^{2\pi} \delta(\phi_A - \phi_0) d\phi_A = 1$. The impulse function $\delta(r_A - r_0)$ has units of inverse meters and $\delta(\phi_A - \phi_0)$ has units of inverse radians. Therefore, with the use of (8.1-77) and the principle of superposition, the complex frequency response (complex aperture function) of the planar array shown in Fig. 8.1-6 can be expressed as the sum of the complex-weighted frequency responses of all the elements in the array as follows:

$$A(f, r_A, \phi_A) = \frac{\mathcal{S}(f)}{r_A} \sum_{m=1}^M \sum_{n=1}^N c_{mn}(f) \delta(r_A - r_m) \delta(\phi_A - \phi_n), \quad (8.1-78)$$

where M is the total number (even or odd) of concentric circular arrays, N is the total number (even or odd) of omnidirectional point-elements per circular array,

$$c_{mn}(f) = a_{mn}(f) \exp[+j\theta_{mn}(f)] \quad (8.1-79)$$

is the frequency-dependent, complex weight associated with element (m, n) , where $a_{mn}(f)$ is a real, frequency-dependent, dimensionless, amplitude weight, and $\theta_{mn}(f)$ is a real, frequency-dependent, phase weight in radians, and (r_m, ϕ_n) are the polar coordinates of the center of element (m, n) . Since the elements are equally spaced in the r and ϕ directions,

$$r_m = m\Delta r, \quad (8.1-80)$$

where

$$\Delta r = a/M \quad (8.1-81)$$

and a is the maximum radial extent of the array in meters, and

$$\phi_n = (n-1)\Delta\phi, \quad (8.1-82)$$

where

$$\Delta\phi = 360^\circ/N. \quad (8.1-83)$$

Substituting (8.1-78) into (8.1-76) yields the following expression for the far-field beam pattern of a planar array of concentric circular arrays of identical, equally-spaced, complex-weighted, omnidirectional point-elements lying in the XY plane:

$$D(f, \theta, \psi) = \mathcal{S}(f) \sum_{m=1}^M \sum_{n=1}^N c_{mn}(f) \exp\left[+j \frac{2\pi r_m}{\lambda} \sin\theta \cos(\psi - \phi_n)\right] \quad (8.1-84)$$

where $\mathcal{S}(f)$ is the complex, element sensitivity function, and the double summation is the dimensionless array factor. Since

$$\cos(\psi - \phi_n) = \cos \psi \cos \phi_n + \sin \psi \sin \phi_n, \quad (8.1-85)$$

(8.1-84) can also be expressed as

$$D(f, u, v) = \mathcal{S}(f) \sum_{m=1}^M \sum_{n=1}^N c_{mn}(f) \exp \left[+j \frac{2\pi}{\lambda} (u x_{mn} + v y_{mn}) \right], \quad (8.1-86)$$

or

$$D(f, f_X, f_Y) = \mathcal{S}(f) \sum_{m=1}^M \sum_{n=1}^N c_{mn}(f) \exp \left[+j 2\pi (f_X x_{mn} + f_Y y_{mn}) \right], \quad (8.1-87)$$

where

$$x_{mn} = r_m \cos \phi_n \quad (8.1-88)$$

and

$$y_{mn} = r_m \sin \phi_n \quad (8.1-89)$$

are the rectangular coordinates of element (m, n) , and spatial frequencies

$$f_X = u/\lambda = \sin \theta \cos \psi / \lambda \quad (8.1-90)$$

and

$$f_Y = v/\lambda = \sin \theta \sin \psi / \lambda. \quad (8.1-91)$$

For the special case of a *single circular array*, $M = 1$, and as a result, $m = 1$ and $r_1 = \Delta r = a$. Therefore, the far-field beam patterns given by (8.1-84), (8.1-86), and (8.1-87) reduce as follows:

$$D(f, \theta, \psi) = \mathcal{S}(f) \sum_{n=1}^N c_n(f) \exp \left[+j \frac{2\pi a}{\lambda} \sin \theta \cos(\psi - \phi_n) \right] \quad (8.1-92)$$

$$D(f, u, v) = \mathcal{S}(f) \sum_{n=1}^N c_n(f) \exp \left[+j \frac{2\pi}{\lambda} (u x_n + v y_n) \right], \quad (8.1-93)$$

and

$$D(f, f_X, f_Y) = \mathcal{S}(f) \sum_{n=1}^N c_n(f) \exp \left[+j 2\pi (f_X x_n + f_Y y_n) \right], \quad (8.1-94)$$

respectively, where

$$x_n = a \cos \phi_n \quad (8.1-95)$$

and

$$y_n = a \sin \phi_n. \quad (8.1-96)$$



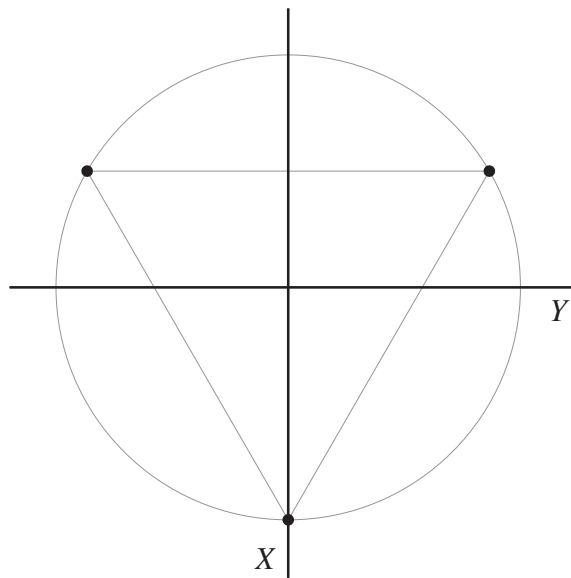


Figure 8.1-7 A triplet circular array.

Example 8.1-7 Triplet – Cardioid Beam Pattern

A special case of a single circular array is a *triplet*. A triplet is composed of three identical, equally-spaced, complex-weighted, omnidirectional point-elements that form an equilateral triangle (see Fig. 8.1-7). Substituting (8.1-95), (8.1-96), and $N = 3$ into (8.1-93) yields the following *unnormalized*, far-field beam pattern of a triplet lying in the XY plane:

$$D(f, u, v) = \mathcal{S}(f) \sum_{n=1}^3 c_n(f) \exp[+jka(u \cos \phi_n + v \sin \phi_n)], \quad (8.1-97)$$

where

$$ka = 2\pi a / \lambda, \quad (8.1-98)$$

a is the radius of the circular array in meters, and by substituting (8.1-83) and $N = 3$ into (8.1-82),

$$\phi_n = (n - 1)120^\circ, \quad n = 1, 2, 3. \quad (8.1-99)$$

Evaluating (8.1-99) yields $\phi_1 = 0^\circ$, $\phi_2 = 120^\circ$, and $\phi_3 = 240^\circ$. Therefore, (8.1-97) can be rewritten as

$$D(f, u, v) = \mathcal{S}(f) \left[c_1(f) \exp(+jka u) + c_2(f) \exp\left[-j \frac{ka}{2} (u - \sqrt{3}v)\right] + c_3(f) \exp\left[-j \frac{ka}{2} (u + \sqrt{3}v)\right] \right], \quad (8.1-100)$$

where $\mathcal{S}(f)$ is the complex, element sensitivity function.

In order to create a *cardioid* (heart-shaped) beam pattern from a triplet, set complex weight

$$c_1(f) = -[c_2(f) + c_3(f)] \exp\left[+j\frac{3}{2}ka\right]. \quad (8.1-101)$$

If we let

$$c_3(f) = c_2(f) = a(f), \quad (8.1-102)$$

where $a(f)$ is a real, frequency-dependent, dimensionless, amplitude weight; and

$$ka = \pi/3, \quad (8.1-103)$$

then

$$c_1(f) = -2a(f)\exp(+j\pi/2) = -j2a(f), \quad (8.1-104)$$

or

$$c_1(f) = 2a(f)\exp(-j\pi/2). \quad (8.1-105)$$

Substituting (8.1-102), (8.1-103), and (8.1-105) into (8.1-100) yields the *unnormalized, cardioid*, far-field beam pattern of a triplet lying in the *XY* plane:

$$D(f, u, v) = 2a(f)\mathcal{S}(f)\exp\left(+j\frac{\pi}{3}u\right) \left[\exp\left(-j\frac{\pi}{2}u\right) \cos\left(\frac{\sqrt{3}}{6}\pi v\right) - j \right]$$

(8.1-106)

The magnitude of the beam pattern given by (8.1-106) is

$$|D(f, u, v)| = 2|a(f)| |\mathcal{S}(f)| \left| \exp\left(-j\frac{\pi}{2}u\right) \cos\left(\frac{\sqrt{3}}{6}\pi v\right) - j \right|, \quad (8.1-107)$$

and since the maximum value of

$$\left| \exp\left(-j\frac{\pi}{2}u\right) \cos\left(\frac{\sqrt{3}}{6}\pi v\right) - j \right|$$

occurs at $u = 1$ and $v = 0$ where

$$\left| \exp\left(-j\frac{\pi}{2}\right) - j \right| = |-j2| = 2, \quad (8.1-108)$$

the normalization factor is

$$D_{\max} = \max |D(f, u, v)| = 4 |\mathbf{a}(f)| |\mathcal{S}(f)|. \quad (8.1-109)$$

Dividing (8.1-107) by (8.1-109) yields the following expression for the magnitude of the *normalized, cardioid*, far-field beam pattern of a triplet lying in the *XY* plane:

$$|D_N(f, u, v)| = \frac{1}{2} \left| \exp\left(-j \frac{\pi}{2} u\right) \cos\left(\frac{\sqrt{3}}{6} \pi v\right) - j \right| \quad (8.1-110)$$

where $|D_N(f, 1, 0)| = 1$. Substituting $u = \sin \theta \cos \psi$ and $v = \sin \theta \sin \psi$ into (8.1-110) yields

$$|D_N(f, \theta, \psi)| = \frac{1}{2} \left| \exp\left(-j \frac{\pi}{2} \sin \theta \cos \psi\right) \cos\left(\frac{\sqrt{3}}{6} \pi \sin \theta \sin \psi\right) - j \right|, \quad (8.1-111)$$

and by setting $\theta = 90^\circ$ in (8.1-111), we obtain

$$|D_N(f, 90^\circ, \psi)| = \frac{1}{2} \left| \exp\left(-j \frac{\pi}{2} \cos \psi\right) \cos\left(\frac{\sqrt{3}}{6} \pi \sin \psi\right) - j \right|, \quad (8.1-112)$$

which is the magnitude of the normalized, *horizontal*, far-field beam pattern in the *XY* plane (see Fig. 8.1-8).

In the *XZ* plane, $\psi = 0^\circ$ (positive *X* axis) or $\psi = 180^\circ$ (negative *X* axis). Therefore, the magnitude of the normalized, *vertical*, far-field beam pattern in the *XZ* plane can be obtained by evaluating (8.1-111) at $\psi = 0^\circ$ and $\psi = 180^\circ$ for $0^\circ \leq \theta \leq 180^\circ$, that is,

$$|D_N(f, \theta, 0^\circ)| = \frac{1}{2} \left| \exp\left(-j \frac{\pi}{2} \sin \theta\right) - j \right|, \quad 0^\circ \leq \theta \leq 180^\circ, \quad (8.1-113)$$

and

$$|D_N(f, \theta, 180^\circ)| = \frac{1}{2} \left| \exp\left(+j \frac{\pi}{2} \sin \theta\right) - j \right|, \quad 0^\circ \leq \theta \leq 180^\circ. \quad (8.1-114)$$

Combining (8.1-113) and (8.1-114) yields Fig. 8.1-9.

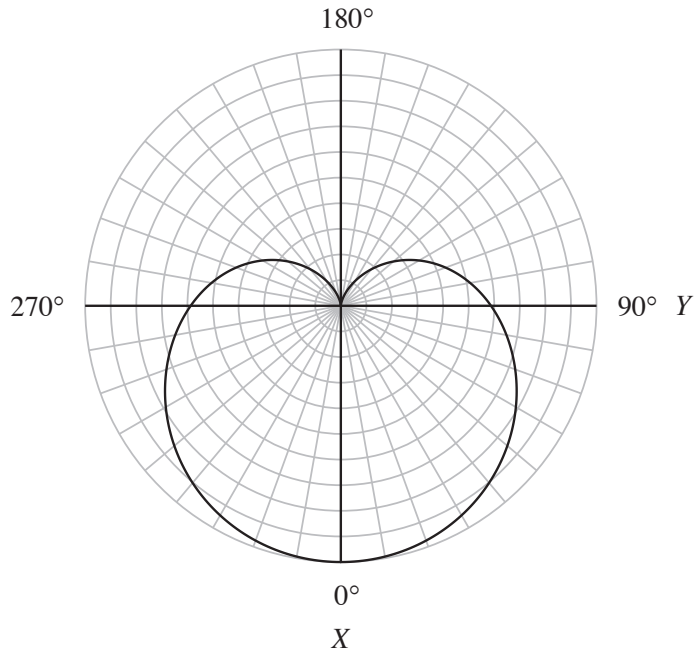


Figure 8.1-8 Polar plot, as a function of the azimuthal (bearing) angle ψ , of the magnitude of the normalized, horizontal, far-field beam pattern of a triplet given by (8.1-112).

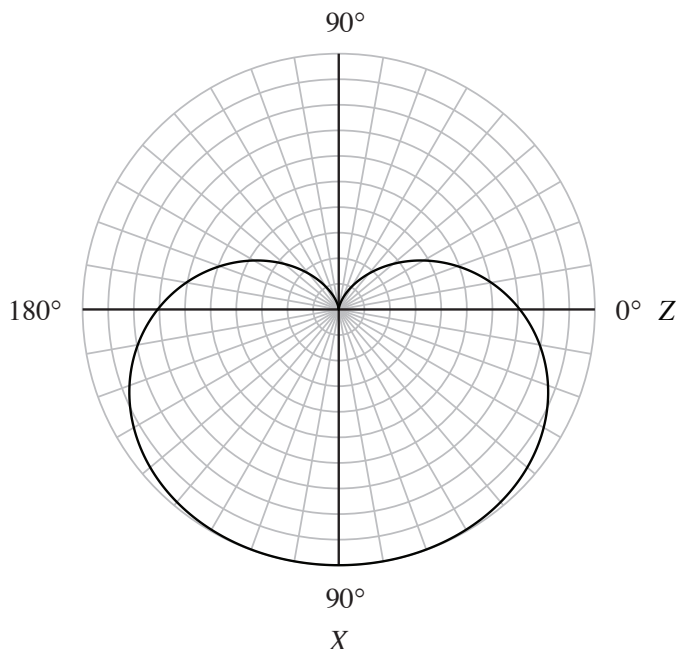


Figure 8.1-9 Polar plot, as a function of the vertical angle θ , of the magnitude of the normalized, vertical, far-field beam pattern of a triplet given by combining (8.1-113) and (8.1-114).

If the complex weight

$$c_l(f) = 2 a(f) \exp(+j\pi/2), \quad (8.1-115)$$

then the *unnormalized, cardioid*, far-field beam pattern of a triplet lying in the XY plane is given by

$$D(f, u, v) = 2 a(f) \mathcal{S}(f) \exp\left(+j\frac{\pi}{3}u\right) \left[\exp\left(-j\frac{\pi}{2}u\right) \cos\left(\frac{\sqrt{3}}{6}\pi v\right) + j \right]$$

(8.1-116)

and the main lobes of the horizontal and vertical beam patterns are aligned along the negative X axis instead of the positive X axis (see Figs. 8.1-10 and 8.1-11). One solution to the port/starboard (left/right) ambiguity problem associated with linear arrays is a linear array composed of triplet elements perpendicular to the array axis (see Example 9.1-2). ■

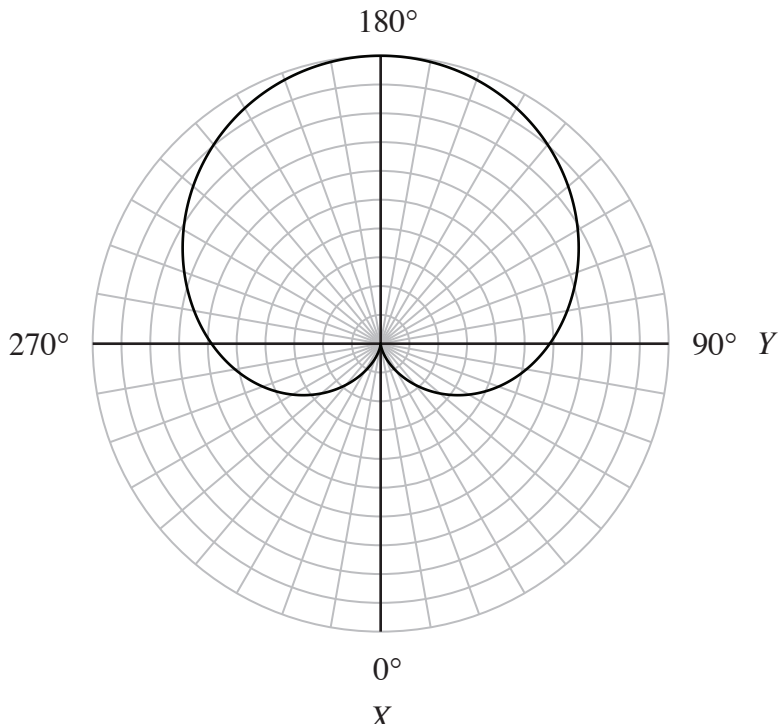


Figure 8.1-10 Polar plot, as a function of the azimuthal (bearing) angle ψ , of the magnitude of the normalized, horizontal, far-field beam pattern of (8.1-116) for a triplet.

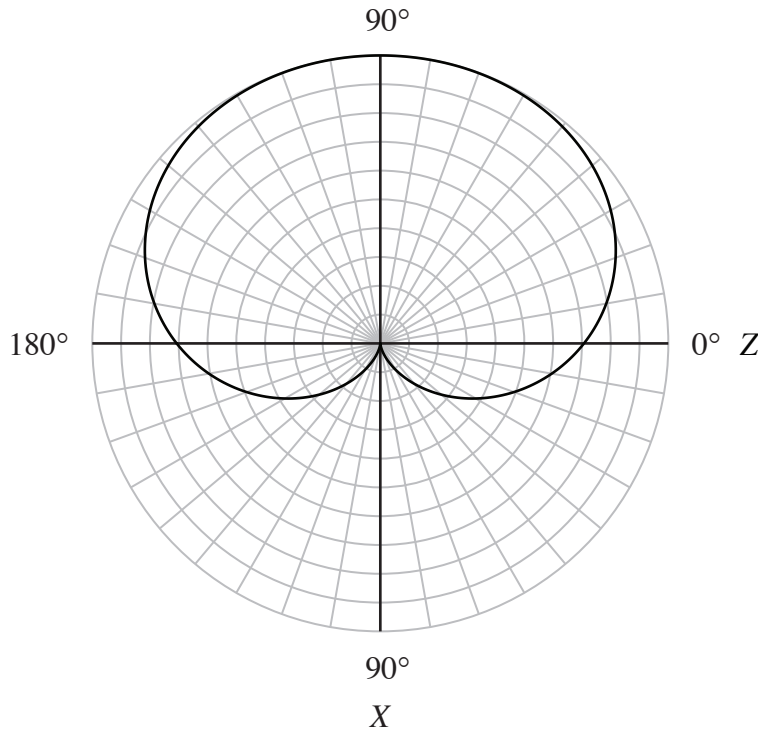


Figure 8.1-11 Polar plot, as a function of the vertical angle θ , of the magnitude of the normalized, vertical, far-field beam pattern of (8.1-116) for a triplet.

Example 8.1-8 Linear Array in a Plane

In this example we shall derive the far-field beam pattern of a linear array composed of an odd number M of unevenly-spaced, complex-weighted elements lying in the XY plane (see Fig. 8.1-12). For example, the elements can be omnidirectional point-elements, rectangular pistons, or circular pistons. If the elements are *not* identical, that is, if each element has a different complex frequency response, and if the elements are *not* equally spaced, as shown in Fig. 8.1-12, then by using the principle of superposition, the complex frequency response (complex aperture function) of this array can be expressed as the sum of the complex-weighted frequency responses of all the elements in the array as follows:

$$A(f, x_A, y_A) = \sum_{m=-M'}^{M'} c_m(f) e_m(f, x_A - x_m, y_A - y_m), \quad (8.1-117)$$

where

$$M' = (M - 1)/2, \quad (8.1-118)$$

$$c_m(f) = a_m(f) \exp[+j\theta_m(f)] \quad (8.1-119)$$

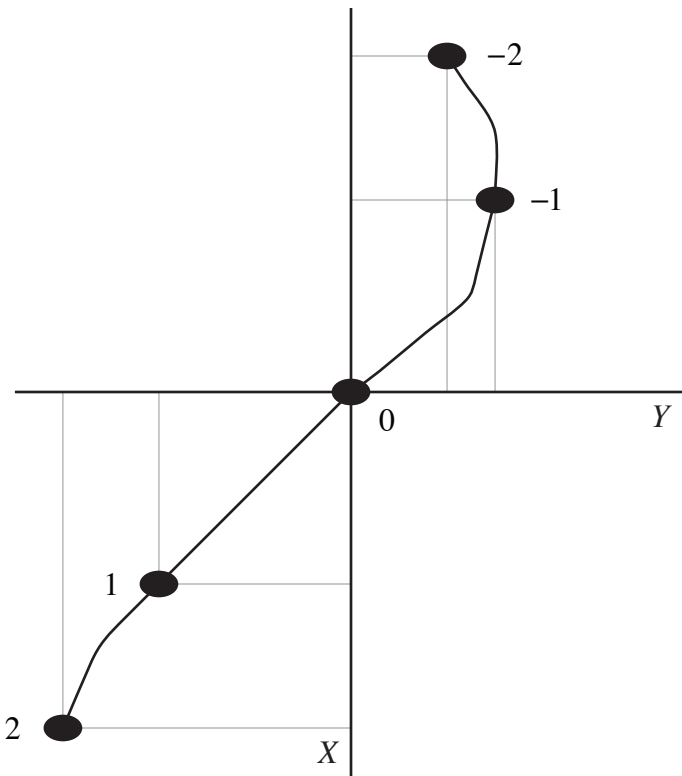


Figure 8.1-12 Linear array composed of an odd number of unevenly-spaced elements lying in the XY plane. Also shown are the element numbers.

is the frequency-dependent, complex weight associated with element m , $a_m(f)$ is a real, frequency-dependent, dimensionless, amplitude weight, $\theta_m(f)$ is a real, frequency-dependent, phase weight in radians, $e_m(f, x_A, y_A)$ is the complex frequency response (complex aperture function) of element m , also known as the element function, and x_m and y_m are the x and y coordinates of the center of element m . Note that $x_0 = 0$ and $y_0 = 0$ because element $m = 0$ is centered at the origin of the coordinate system.

Taking the two-dimensional spatial Fourier transform of (8.1-117) with respect to x_A and y_A yields the following expression for the far-field beam pattern:

$$D(f, f_X, f_Y) = \sum_{m=-M'}^{M'} c_m(f) E_m(f, f_X, f_Y) \exp[j2\pi(f_X x_m + f_Y y_m)]$$

(8.1-120)

where

$$F_{x_A} F_{y_A} \{ e_m(f, x_A - x_m, y_A - y_m) \} = E_m(f, f_X, f_Y) \exp[+j2\pi(f_X x_m + f_Y y_m)] \quad (8.1-121)$$

and

$$E_m(f, f_X, f_Y) = F_{x_A} F_{y_A} \{ e_m(f, x_A, y_A) \} \quad (8.1-122)$$

is the far-field beam pattern of element (electroacoustic transducer) m . If all the elements in the array are *identical* (i.e., all the elements have the same complex frequency response), but still *not* equally spaced, then (8.1-120) reduces to the Product Theorem [see (8.1-12)]

$$D(f, f_X, f_Y) = E(f, f_X, f_Y) S(f, f_X, f_Y) \quad (8.1-123)$$

where

$$E(f, f_X, f_Y) = F_{x_A} F_{y_A} \{ e(f, x_A, y_A) \} \quad (8.1-124)$$

is the far-field beam pattern of *one* of the identical elements in the array, but now

$$S(f, f_X, f_Y) = \sum_{m=-M'}^{M'} c_m(f) \exp[+j2\pi(f_X x_m + f_Y y_m)] \quad (8.1-125)$$

Note that the dimensionless array factor $S(f, f_X, f_Y)$ given by (8.1-125) for a *linear* array in the XY plane is different than $S(f, f_X, f_Y)$ given by (8.1-14) for a planar array in the XY plane. ■

8.2 The Phased Array – Beam Steering

Consider a planar array composed of an odd number $M \times N$ of identical, unevenly-spaced, complex-weighted, omnidirectional point-elements lying in the XY plane, where M and N are the total odd number of elements in the X and Y directions, respectively. From the Product Theorem for an odd number of elements, the far-field beam pattern of this array is given by [see (8.1-19)]

$$D(f, f_X, f_Y) = \mathcal{S}(f) S(f, f_X, f_Y), \quad (8.2-1)$$

where $\mathcal{S}(f)$ is the complex, element sensitivity function (see [Table 8.1-2](#) and [Appendix 6B](#)),

$$S(f, f_X, f_Y) = \sum_{m=-M'}^{M'} \sum_{n=-N'}^{N'} c_{mn}(f) \exp[+j2\pi(f_X x_{mn} + f_Y y_{mn})], \quad (8.2-2)$$

$$c_{mn}(f) = a_{mn}(f) \exp[+j\theta_{mn}(f)], \quad (8.2-3)$$

$$M' = (M - 1)/2, \quad (8.2-4)$$

and

$$N' = (N - 1)/2. \quad (8.2-5)$$

Let $D(f, f_X, f_Y)$ be the far-field beam pattern of the array when it is only amplitude weighted (i.e., $\theta_{mn}(f) = 0 \quad \forall m \text{ and } n$), and let $D'(f, f_X, f_Y)$ be the far-field beam pattern of the array when it is complex weighted. Therefore,

$$D(f, f_X, f_Y) = \mathcal{S}(f) \sum_{m=-M'}^{M'} \sum_{n=-N'}^{N'} a_{mn}(f) \exp[j2\pi(f_X x_{mn} + f_Y y_{mn})] \quad (8.2-6)$$

and

$$D'(f, f_X, f_Y) = \mathcal{S}(f) \sum_{m=-M'}^{M'} \sum_{n=-N'}^{N'} a_{mn}(f) \exp\left\{j\left[2\pi f_X x_{mn} + 2\pi f_Y y_{mn} + \theta_{mn}(f)\right]\right\}. \quad (8.2-7)$$

We already know from planar aperture theory that in order to do beam steering, there must be a linear phase response across the surface of the aperture in both the X and Y directions (see [Section 3.4](#)). A set of linear phase weights that will produce a linear phase response across the surface of the planar array under discussion in both the X and Y directions is given by

$$\theta_{mn}(f) = -2\pi f'_X x_{mn} - 2\pi f'_Y y_{mn}, \quad m = -M', \dots, 0, \dots, M' \\ n = -N', \dots, 0, \dots, N'$$

(8.2-8)

where

$$f'_X = u'/\lambda = \sin\theta' \cos\psi'/\lambda$$

(8.2-9)

and

$$f'_Y = v'/\lambda = \sin\theta' \sin\psi'/\lambda$$

(8.2-10)

If the elements are *equally spaced*, then $x_{mn} = md_X$ and $y_{mn} = nd_Y$ [see (8.1-22) and (8.1-23)], and in order to avoid grating lobes for all possible directions of beam steering, $d_X < \lambda_{\min}/2$ and $d_Y < \lambda_{\min}/2$, where λ_{\min} is the minimum wavelength associated with the maximum frequency $f_{\max} = c/\lambda_{\min}$ in hertz (see [Subsection 6.5.1](#)). Compare (8.2-8) through (8.2-10) with (3.4-3) through (3.4-5). If (8.2-8) is substituted into (8.2-7), then

$$D'(f, f_X, f_Y) = \mathcal{S}(f) \sum_{m=-M'}^{M'} \sum_{n=-N'}^{N'} a_{mn}(f) \exp \left\{ +j2\pi \left[(f_X - f'_X)x_{mn} + (f_Y - f'_Y)y_{mn} \right] \right\}, \quad (8.2-11)$$

and by comparing (8.2-11) with (8.2-6),

$$D'(f, f_X, f_Y) = D(f, f_X - f'_X, f_Y - f'_Y). \quad (8.2-12)$$

Since spatial frequencies

$$f_X = u/\lambda = \sin\theta \cos\psi/\lambda \quad (8.2-13)$$

and

$$f_Y = v/\lambda = \sin\theta \sin\psi/\lambda, \quad (8.2-14)$$

(8.2-12) can also be expressed as

$$D'(f, u, v) = D(f, u - u', v - v'). \quad (8.2-15)$$

Equation (8.2-15) indicates that a set of linear phase weights applied across the surface of the array in both the X and Y directions will steer the far-field beam pattern $D(f, u, v)$ of a set of amplitude weights in the direction $u = u'$ and $v = v'$ in direction-cosine space, which is equivalent to steering (tilting) the beam pattern to $\theta = \theta'$ and $\psi = \psi'$ [see (8.2-9) and (8.2-10)]. Equal spacing of the elements is *not* required in order to do beam steering. Equation (8.2-15) also indicates that the far-field beam pattern $D'(f, u, v)$ is simply a translated or shifted version of $D(f, u, v)$ in the uv plane, implying that the shape and beamwidth of the mainlobe of the beam pattern remain unchanged. However, recall from linear aperture theory, that when a beam pattern is steered, the shape and beamwidth of the mainlobe of the beam pattern do change when the magnitude of the beam pattern is plotted as a function of the spherical angles θ and ψ (see [Section 2.5](#)).

Finally, note that a phase weight $\theta_{mn}(f)$ in radians is equivalent to a *time delay* τ'_{mn} in seconds, that is,

$$\theta_{mn}(f) \triangleq -2\pi f \tau'_{mn}, \quad (8.2-16)$$

or

$$\tau'_{mn} = -\theta_{mn}(f)/(2\pi f). \quad (8.2-17)$$

Substituting (8.2-8) through (8.2-10) into (8.2-17) yields

$$\tau'_{mn} = \frac{u'}{c} x_{mn} + \frac{v'}{c} y_{mn}, \quad m = -M', \dots, 0, \dots, M' \\ n = -N', \dots, 0, \dots, N' \quad (8.2-18)$$

where $c = f\lambda$. The phase weights given by (8.2-8) or, equivalently, the time delays given by (8.2-18) are implemented by using the beamforming procedure shown in Fig. 8.2-1. Note that the amplitude weight a_{mn} in Fig. 8.2-1 is *not* a function of frequency.

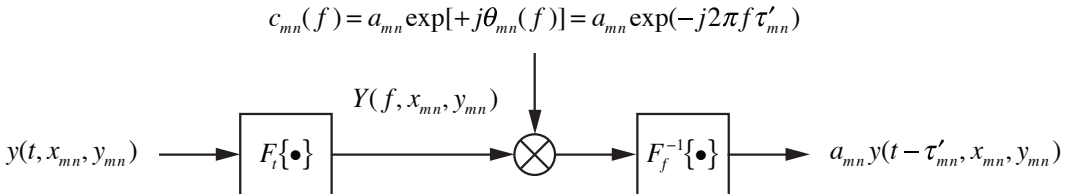


Figure 8.2-1 Beamforming. Implementing a complex weight (amplitude and phase weights) using forward and inverse Fourier transforms.

In Fig. 8.2-1, $y(t, x_{mn}, y_{mn})$ is the output electrical signal from element (m, n) in a planar array. The complex weight $c_{mn}(f)$ is just a complex number in a computer program. The expression $F_t\{\cdot\}$ represents a forward Fourier transform with respect to time t , and $F_f^{-1}\{\cdot\}$ represents an inverse Fourier transform with respect to frequency f . In practical applications, the forward and inverse Fourier transforms are computed using forward and inverse *discrete Fourier transforms* (DFTs), which can be evaluated very quickly by using forward and inverse *fast-Fourier-transform* (FFT) algorithms. This is known as *digital beamforming* or *FFT beamforming*. Since the phase weight $\theta_{mn}(f)$ is a function of frequency f , an appropriate phase weight must be applied to *each* frequency component contained in the complex frequency spectrum $Y(f, x_{mn}, y_{mn})$ shown in Fig. 8.2-1 in order to produce the correct time delay τ'_{mn} . This must be done at each element in a planar array.

Example 8.2-1 Twin-Line Planar Array

One solution to the port/starboard (left/right) ambiguity problem associated with linear arrays is a twin-line planar array. Consider a twin-line planar array of identical, complex-weighted, omnidirectional point-elements lying in the XY plane as shown in Fig. 8.2-2. The elements are equally spaced in the X direction, and equally spaced in the Y direction. If the complex weights $c_{mn}(f)$ are separable [see (8.1-40)], and since $E(f, f_X, f_Y) = \mathcal{S}(f)$, where $\mathcal{S}(f)$ is the complex, element sensitivity function, then the unnormalized, far-field beam pattern of this array is given by the Product Theorem [see (8.1-46)]

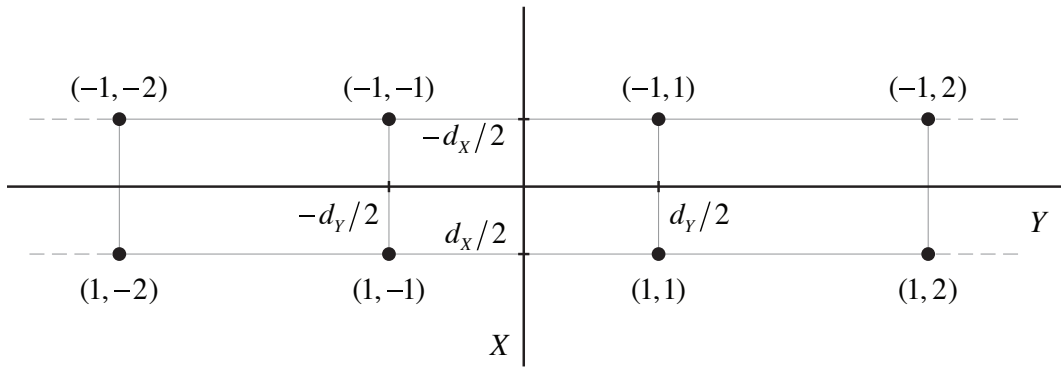


Figure 8.2-2 Top view of a twin-line planar array of identical, omnidirectional point-elements lying in the XY plane. The positive Z axis points toward the surface. Also shown are the element numbers (m, n) .

$$D(f, f_X, f_Y) = \mathcal{S}(f) S_X(f, f_X) S_Y(f, f_Y), \quad (8.2-19)$$

where

$$S_X(f, f_X) = c_{-1}(f) \exp(+j2\pi f_X x_{-1}) + c_1(f) \exp(+j2\pi f_X x_1) \quad (8.2-20)$$

since there are two elements in the X direction, and

$$S_Y(f, f_Y) = \sum_{n=1}^{N/2} [w_{-n}(f) \exp(+j2\pi f_Y y_{-n}) + w_n(f) \exp(+j2\pi f_Y y_n)], \quad (8.2-21)$$

where N is the total *even* number of elements *per line* in the Y direction [see (6.1-12)].

If

$$c_{-1}(f) = c_1^*(f), \quad (8.2-22)$$

and since

$$x_1 = d_X/2 \quad (8.2-23)$$

and

$$x_{-1} = -x_1, \quad (8.2-24)$$

then (8.2-20) reduces to [see (6.1-28)]

$$S_X(f, f_X) = 2a_1(f) \cos[\pi f_X d_X + \theta_1(f)], \quad (8.2-25)$$

where the amplitude weights in the X direction

$$a_{-1}(f) = a_1(f), \quad (8.2-26)$$

and the phase weights in the X direction

$$\theta_{-l}(f) = -\theta_l(f). \quad (8.2-27)$$

In order to do beam steering, let

$$\theta_l(f) = -\pi f'_X d_X, \quad (8.2-28)$$

where f'_X is given by (8.2-9). Substituting (8.2-28) into (8.2-25) yields

$$S_X(f, f_X) = 2a_1(f)\cos[\pi(f_X - f'_X)d_X]. \quad (8.2-29)$$

Similarly, if

$$w_{-n}(f) = w_n^*(f), \quad n = 1, 2, \dots, N/2, \quad (8.2-30)$$

and since

$$y_n = (n - 0.5)d_Y, \quad n = 1, 2, \dots, N/2, \quad (8.2-31)$$

and

$$y_{-n} = -y_n, \quad n = 1, 2, \dots, N/2, \quad (8.2-32)$$

then (8.2-21) reduces to [see (6.1-28)]

$$S_Y(f, f_Y) = 2 \sum_{n=1}^{N/2} b_n(f) \cos[2\pi f_Y(n - 0.5)d_Y + \phi_n(f)], \quad (8.2-33)$$

where the amplitude weights in the Y direction

$$b_{-n}(f) = b_n(f), \quad n = 1, 2, \dots, N/2, \quad (8.2-34)$$

and the phase weights in the Y direction

$$\phi_{-n}(f) = -\phi_n(f), \quad n = 1, 2, \dots, N/2. \quad (8.2-35)$$

In order to do beam steering, let

$$\phi_n(f) = -2\pi f'_Y(n - 0.5)d_Y, \quad (8.2-36)$$

where f'_Y is given by (8.2-10). Substituting (8.2-36) into (8.2-33) yields

$$S_Y(f, f_Y) = 2 \sum_{n=1}^{N/2} b_n(f) \cos[2\pi(f_Y - f'_Y)(n - 0.5)d_Y]. \quad (8.2-37)$$

Substituting the array factors given by (8.2-29) and (8.2-37) into (8.2-19) yields

$$D(f, f_X, f_Y) = 4 a_1(f) \mathcal{S}(f) \cos[\pi(f_X - f'_X) d_X] \times \sum_{n=1}^{N/2} b_n(f) \cos[2\pi(f_Y - f'_Y)(n - 0.5) d_Y], \quad (8.2-38)$$

and by substituting (8.2-9), (8.2-10), (8.2-13), and (8.2-14) into (8.2-38), we obtain

$$D(f, u, v) = 4 a_1(f) \mathcal{S}(f) \cos[\pi(u - u') d_X / \lambda] \times \sum_{n=1}^{N/2} b_n(f) \cos[2\pi(v - v')(n - 0.5) d_Y / \lambda]. \quad (8.2-39)$$

If the interelement spacings

$$d_X = \lambda / 4 \quad (8.2-40)$$

and

$$d_Y = \lambda / 2, \quad (8.2-41)$$

then (8.2-39) reduces to

$$D(f, u, v) = 4 a_1(f) \mathcal{S}(f) \cos[\pi(u - u') / 4] \sum_{n=1}^{N/2} b_n(f) \cos[\pi(v - v')(n - 0.5)]$$

(8.2-42)

Equation (8.2-42) is the *unnormalized*, far-field beam pattern of a twin-line planar array lying in the XY plane with interelement spacings given by (8.2-40) and (8.2-41), where $\mathcal{S}(f)$ is the complex, element sensitivity function.

The magnitude of the far-field beam pattern given by (8.2-42) is

$$|D(f, u, v)| = 4 |a_1(f)| |\mathcal{S}(f)| \left| \cos[\pi(u - u') / 4] \right| \left| \sum_{n=1}^{N/2} b_n(f) \cos[\pi(v - v')(n - 0.5)] \right|, \quad (8.2-43)$$

and since

$$|D(f, u', v')| = 4 |a_1(f)| |\mathcal{S}(f)| \left| \sum_{n=1}^{N/2} b_n(f) \right|, \quad (8.2-44)$$

if the amplitude weights

$$b_n(f) > 0, \quad n = 1, 2, \dots, N/2, \quad (8.2-45)$$

then the normalization factor is

$$D_{\max} = \max |D(f, u, v)| = 4 |a_1(f)| |\mathcal{S}(f)| \sum_{n=1}^{N/2} b_n(f). \quad (8.2-46)$$

Dividing (8.2-43) by (8.2-46) yields the following expression for the magnitude of the *normalized*, far-field beam pattern of a twin-line planar array lying in the XY plane:

$$\boxed{|D_N(f, u, v)| = \left| \cos[\pi(u - u')/4] \right| \frac{\left| \sum_{n=1}^{N/2} b_n(f) \cos[\pi(v - v')(n - 0.5)] \right|}{\sum_{n=1}^{N/2} b_n(f)}} \quad (8.2-47)$$

where $|D_N(f, u', v')| = 1$. Equation (8.2-47) can also be expressed as

$$\boxed{|D_N(f, \theta, \psi)| = \left| \cos[\pi(\sin \theta \cos \psi - \sin \theta' \cos \psi')/4] \right| \times \frac{\left| \sum_{n=1}^{N/2} b_n(f) \cos[\pi(\sin \theta \sin \psi - \sin \theta' \sin \psi')(n - 0.5)] \right|}{\sum_{n=1}^{N/2} b_n(f)}}, \quad (8.2-48)$$

and by setting $\theta = 90^\circ$ and $\theta' = 90^\circ$ in (8.2-48), we obtain

$$\boxed{|D_N(f, 90^\circ, \psi)| = \left| \cos[\pi(\cos \psi - \cos \psi')/4] \right| \times \frac{\left| \sum_{n=1}^{N/2} b_n(f) \cos[\pi(\sin \psi - \sin \psi')(n - 0.5)] \right|}{\sum_{n=1}^{N/2} b_n(f)}}, \quad (8.2-49)$$

which is the magnitude of the normalized, *horizontal*, far-field beam pattern in the XY plane (see Figs. 8.2-3 and 8.2-4). If the array is towed in the positive Y direction, then $\psi = 0^\circ$ is broadside on the starboard (right) side of the array, and $\psi = 180^\circ$ is broadside on the port (left) side of the array. Like the cardioid beam patterns in Examples 6.1-3 and 8.1-7, the main lobes of the beam patterns in Figs. 8.2-3 and 8.2-4 exist in a half-space. Another solution to the port/starboard (left/right) ambiguity problem is a linear array composed of triplet elements perpendicular to the array axis (see Example 9.1-2). ■

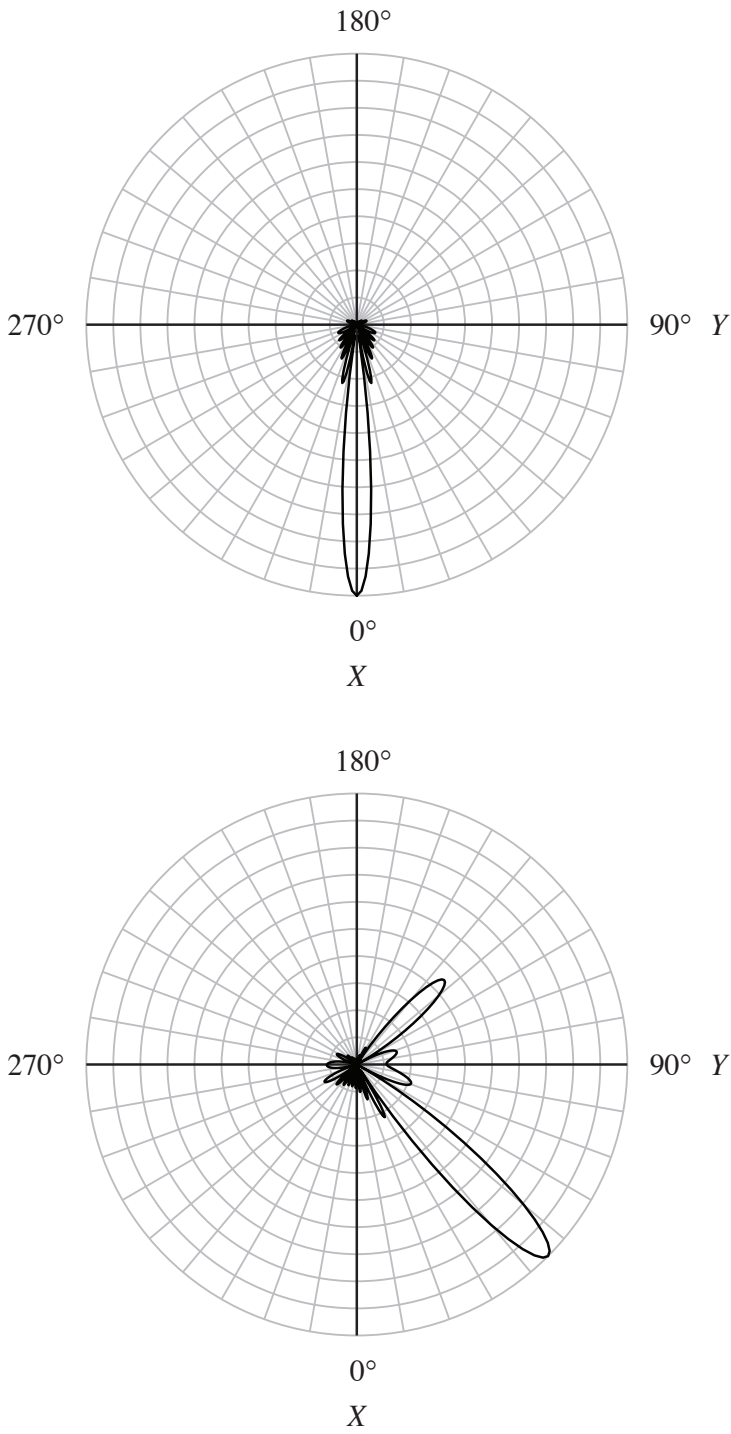


Figure 8.2-3 Polar plot, as a function of the azimuthal (bearing) angle ψ , of the magnitude of the normalized, horizontal, far-field beam pattern of a twin-line planar array given by (8.2-49) for $N = 12$, rectangular amplitude weights, and beam-steer angles (a) $\psi' = 0^\circ$ and (b) $\psi' = 45^\circ$.

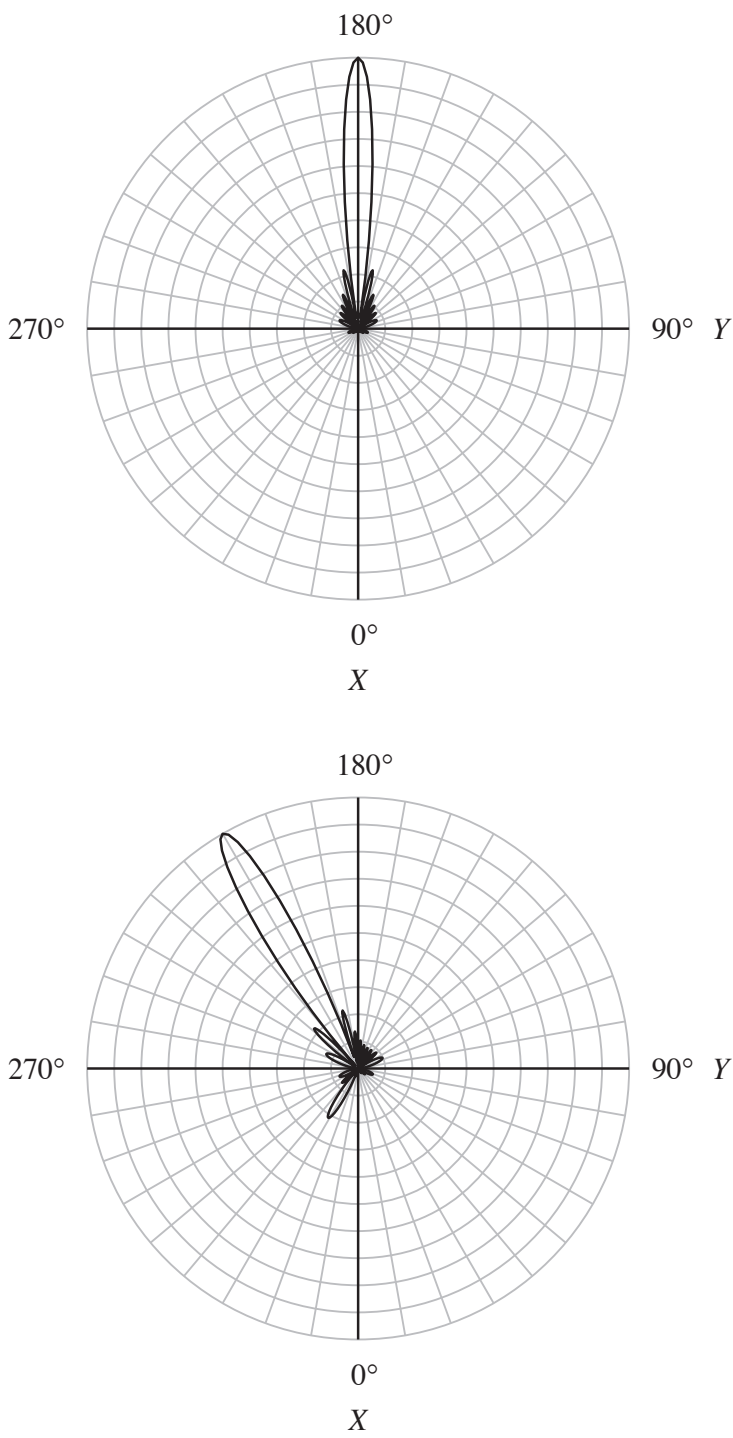


Figure 8.2-4 Polar plot, as a function of the azimuthal (bearing) angle ψ , of the magnitude of the normalized, horizontal, far-field beam pattern of a twin-line planar array given by (8.2-49) for $N = 12$, rectangular amplitude weights, and beam-steer angles (a) $\psi' = 180^\circ$ and (b) $\psi' = 210^\circ$.

8.3 Far-Field Beam Patterns and the Two-Dimensional Spatial Discrete Fourier Transform

In [Section 6.5](#) it was shown that the far-field beam pattern of a linear array composed of an odd number N of identical, equally-spaced, complex-weighted, omnidirectional point-elements lying along the X axis can be computed using a one-dimensional, spatial discrete Fourier transform (DFT). In this section we shall generalize those one-dimensional results and show that the far-field beam pattern of a planar array composed of an odd number $M \times N$ of identical, equally-spaced, complex-weighted, omnidirectional point-elements lying in the XY plane, where M and N are the total odd number of elements in the X and Y directions, respectively, can be computed using a two-dimensional, spatial DFT or, if separable complex weights are used, the product of two, one-dimensional, spatial DFTs. The far-field beam pattern of the aforementioned planar array can be obtained by substituting (8.1-14), (8.1-22), and (8.1-23) into (8.1-19). Doing so yields

$$D(f, f_X, f_Y) = \mathcal{S}(f) \sum_{m=-M'}^{M'} \sum_{n=-N'}^{N'} c_{mn}(f) \exp[j2\pi(f_X m d_X + f_Y n d_Y)], \quad (8.3-1)$$

where $\mathcal{S}(f)$ is the complex, element sensitivity function (see [Table 8.1-2](#) and [Appendix 6B](#)),

$$c_{mn}(f) = a_{mn}(f) \exp[j\theta_{mn}(f)], \quad (8.3-2)$$

$$M' = (M - 1)/2, \quad (8.3-3)$$

and

$$N' = (N - 1)/2. \quad (8.3-4)$$

According to (8.3-1), $D(f, f_X, f_Y)$ is evaluated at continuous values of spatial frequencies f_X and f_Y . Following the procedure in [Section 6.5](#), a more efficient way to compute $D(f, f_X, f_Y)$ is to evaluate it at the following set of discrete values of f_X and f_Y :

$$f_X = r \Delta f_X, \quad r = -M'', \dots, 0, \dots, M'', \quad (8.3-5)$$

and

$$f_Y = s \Delta f_Y, \quad s = -N'', \dots, 0, \dots, N'', \quad (8.3-6)$$

where

$$\Delta f_X = \frac{1}{(M + Z_X) d_X} \leq \frac{1}{M d_X} \quad (8.3-7)$$

and

$$\Delta f_Y = \frac{1}{(N + Z_Y)d_Y} \leq \frac{1}{Nd_Y} \quad (8.3-8)$$

are the spatial-frequency spacings (in cycles per meter) in the X and Y directions, respectively, $Z_X \geq 0$ and $Z_Y \geq 0$ are *positive integers* used for “padding-with-zeros”, d_X and d_Y are the interelement spacings (in meters) in the X and Y directions, respectively,

$$M'' = \begin{cases} (M + Z_X)/2, & M + Z_X \text{ even} \\ (M + Z_X - 1)/2, & M + Z_X \text{ odd} \end{cases} \quad (8.3-9)$$

and

$$N'' = \begin{cases} (N + Z_Y)/2, & N + Z_Y \text{ even} \\ (N + Z_Y - 1)/2, & N + Z_Y \text{ odd.} \end{cases} \quad (8.3-10)$$

Substituting (8.3-5) through (8.3-8) into (8.3-1) yields

$$D(f, r, s) = \mathcal{S}(f) \sum_{m=-M'}^{M'} \sum_{n=-N'}^{N'} c_{mn}(f) W_{M+Z_X}^{rm} W_{N+Z_Y}^{sn}, \quad r = -M'', \dots, 0, \dots, M''$$

$$s = -N'', \dots, 0, \dots, N''$$

(8.3-11)

where the double summation on the right-hand side of (8.3-11) is the *two-dimensional*, spatial DFT of the set of $M \times N$ complex weights $c_{mn}(f)$,

$$W_{M+Z_X} = \exp\left(+j \frac{2\pi}{M + Z_X}\right), \quad (8.3-12)$$

and

$$W_{N+Z_Y} = \exp\left(+j \frac{2\pi}{N + Z_Y}\right). \quad (8.3-13)$$

Equation (8.3-11) can also be expressed as a sequence of two, one-dimensional spatial DFTs as follows:

$$D(f, r, s) = \mathcal{S}(f) \sum_{n=-N'}^{N'} \mathcal{S}_X(f, r, n) W_{N+Z_Y}^{sn}, \quad r = -M'', \dots, 0, \dots, M''$$

$$s = -N'', \dots, 0, \dots, N''$$

(8.3-14)

where

$$\mathcal{S}_X(f, r, n) = \sum_{m=-M'}^{M'} c_{mn}(f) W_{M+Z_X}^{rm}, \quad r = -M'', \dots, 0, \dots, M'' \\ n = -N', \dots, 0, \dots, N' \quad (8.3-15)$$

is directly proportional to the far-field beam pattern of a linear array composed of an odd number M of identical, equally-spaced, complex-weighted, omnidirectional point-elements lying along a line with y coordinate nd_y that is parallel to the X axis.

If separable complex weights are used, then substituting (8.1-55) into (8.3-11) yields

$$D(f, r, s) = \mathcal{S}(f) S_X(f, r) S_Y(f, s), \quad r = -M'', \dots, 0, \dots, M'' \\ s = -N'', \dots, 0, \dots, N'' \quad (8.3-16)$$

where

$$S_X(f, r) = \sum_{m=-M'}^{M'} c_m(f) W_{M+Z_X}^{rm}, \quad r = -M'', \dots, 0, \dots, M'' \quad (8.3-17)$$

and

$$S_Y(f, s) = \sum_{n=-N'}^{N'} w_n(f) W_{N+Z_Y}^{sn}, \quad s = -N'', \dots, 0, \dots, N'' \quad (8.3-18)$$

are one-dimensional, spatial DFTs in the X and Y directions, respectively, where

$$c_m(f) = a_m(f) \exp[+j\theta_m(f)] \quad (8.3-19)$$

is the complex weight in the X direction, and

$$w_n(f) = b_n(f) \exp[+j\phi_n(f)] \quad (8.3-20)$$

is the complex weight in the Y direction. Note that $\mathcal{S}_X(f, r, 0) = S_X(f, r)$ if $c_{m0}(f) = c_m(f)$ [see (8.3-15)].

In order to relate the DFT bin numbers r and s to values of the spherical angles θ and ψ , we first need to derive relationships between bin numbers r and s and the corresponding values of direction cosines u_r and v_s , respectively. Since [see (8.3-5)]

$$f_X = \frac{u}{\lambda} = r \Delta f_X, \quad r = -M'', \dots, 0, \dots, M'', \quad (8.3-21)$$

solving for direction cosine u yields

$$u = u_r = r \lambda \Delta f_X, \quad r = -M'', \dots, 0, \dots, M'', \quad (8.3-22)$$

and by substituting (8.3-7) into (8.3-22), we obtain

$$u_r = \frac{r}{M + Z_X} \frac{\lambda}{d_X}, \quad r = -M'', \dots, 0, \dots, M'' \quad (8.3-23)$$

where M'' is given by (8.3-9). Similarly, since [see (8.3-6)],

$$f_Y = \frac{v}{\lambda} = s \Delta f_Y, \quad s = -N'', \dots, 0, \dots, N'', \quad (8.3-24)$$

solving for direction cosine v yields

$$v = v_s = s \lambda \Delta f_Y, \quad s = -N'', \dots, 0, \dots, N'', \quad (8.3-25)$$

and by substituting (8.3-8) into (8.3-25), we obtain

$$v_s = \frac{s}{N + Z_Y} \frac{\lambda}{d_Y}, \quad s = -N'', \dots, 0, \dots, N'' \quad (8.3-26)$$

where N'' is given by (8.3-10). Substituting $u = u_r$ and $v = v_s$ into (3.2-9) and (3.2-10) yields

$$\theta_{rs} = \sin^{-1} \sqrt{u_r^2 + v_s^2}, \quad \sqrt{u_r^2 + v_s^2} \leq 1 \quad (8.3-27)$$

and

$$\psi_{rs} = \tan^{-1}(v_s/u_r) \quad (8.3-28)$$

respectively. Equations (8.3-27) and (8.3-28) are used to compute values for the spherical angles θ and ψ at DFT bins r and s . As discussed in [Section 3.2](#), only those (u_r, v_s) coordinates inside or on the unit circle shown in [Fig. 3.2-3](#) can be used for computing θ_{rs} and ψ_{rs} . Also, by taking into account the signs (quadrant) of the (u_r, v_s) coordinates, one may have to add either 180° or 360° to the value

obtained from (8.3-28) so that ψ_{rs} has the correct value (see [Table 3.2-1](#)).

If we let δu be the direction cosine u bin spacing, then by using (8.3-23)

$$\delta u = u_r - u_{r-1} = \frac{1}{M + Z_x} \frac{\lambda}{d_x}. \quad (8.3-29)$$

Solving for Z_x using (8.3-29) yields

$$Z_x = \frac{1}{\delta u} \frac{\lambda}{d_x} - M \quad (8.3-30)$$

Equation (8.3-30) is used to solve for the value of Z_x that is required in order to obtain a desired direction-cosine bin spacing δu . Similarly, if we let δv be the direction cosine v bin spacing, then by using (8.3-26)

$$\delta v = v_s - v_{s-1} = \frac{1}{N + Z_y} \frac{\lambda}{d_y}. \quad (8.3-31)$$

Solving for Z_y using (8.3-31) yields

$$Z_y = \frac{1}{\delta v} \frac{\lambda}{d_y} - N \quad (8.3-32)$$

Equation (8.3-32) is used to solve for the value of Z_y that is required in order to obtain a desired direction-cosine bin spacing δv . See [Section 6.5](#) for more discussion on *folding bins*, “padding-with-zeros”, and the *periodicity* of the DFT.

The *normalized*, far-field beam pattern $D_N(f, r, s)$ is given by

$$D_N(f, r, s) = D(f, r, s) / D_{\max}, \quad (8.3-33)$$

where $D(f, r, s)$ is the unnormalized, far-field beam pattern given by (8.3-11), and if $a_{mn}(f) > 0 \forall m$ and n , then

$$D_{\max} = \max |D(f, r, s)| = |\mathcal{S}(f)| \sum_{m=-M'}^{M'} \sum_{n=-N'}^{N'} a_{mn}(f) \quad (8.3-34)$$

is the normalization factor [use the procedure in [Appendix 6A](#) for N odd to obtain (8.3-34)]. Therefore, dividing the magnitude of (8.3-11) by (8.3-34) yields

$$\boxed{|D_N(f, r, s)| = \frac{\left| \sum_{m=-M'}^{M'} \sum_{n=-N'}^{N'} c_{mn}(f) W_{M+Z_X}^{rm} W_{N+Z_Y}^{sn} \right|}{\sum_{m=-M'}^{M'} \sum_{n=-N'}^{N'} a_{mn}(f)}}, \quad \begin{aligned} r &= -M'', \dots, 0, \dots, M'' \\ s &= -N'', \dots, 0, \dots, N'' \end{aligned}$$

(8.3-35)

8.4 The Near-Field Beam Pattern of a Planar Array

As was mentioned at the beginning of [Section 8.1](#), a planar array is an example of a planar aperture. Therefore, the near-field beam pattern (directivity function) of a planar array lying in the XY plane is given by the following two-dimensional spatial Fresnel transform (see [Section 3.5](#)):

$$\begin{aligned} \mathcal{D}(f, r, f_X, f_Y) &= F_{x_A} F_{y_A} \left\{ A(f, x_A, y_A) \exp \left[-j \frac{k}{2r} (x_A^2 + y_A^2) \right] \right\} \\ &= \int_{-\infty}^{\infty} \int_{-\infty}^{\infty} A(f, x_A, y_A) \exp \left[-j \frac{k}{2r} (x_A^2 + y_A^2) \right] \times \quad (8.4-1) \\ &\quad \exp [+j 2\pi (f_X x_A + f_Y y_A)] dx_A dy_A, \end{aligned}$$

where $A(f, x_A, y_A)$ is the complex frequency response (complex aperture function) of the planar array,

$$k = 2\pi f / c = 2\pi / \lambda \quad (8.4-2)$$

is the wavenumber in radians per meter, and

$$f_X = u / \lambda = \sin \theta \cos \psi / \lambda \quad (8.4-3)$$

and

$$f_Y = v / \lambda = \sin \theta \sin \psi / \lambda \quad (8.4-4)$$

are spatial frequencies in the X and Y directions, respectively, with units of cycles per meter. Since f_X and f_Y can be expressed in terms of the spherical angles θ and ψ , the near-field beam pattern can ultimately be expressed as a function of frequency f , the range r to a field point, and the spherical angles θ and ψ , that is, $\mathcal{D}(f, r, f_X, f_Y) \rightarrow \mathcal{D}(f, r, \theta, \psi)$. We shall consider a field point to be in the Fresnel (near-field) region of an array if the Fresnel angle criterion given by either (1.2-35) or (1.2-91) is satisfied, and the range r to the field point – as

measured from the center of the array – satisfies the Fresnel range criterion given by

$$1.356R_A < r < \pi R_A^2 / \lambda, \quad (8.4-5)$$

where R_A is the maximum radial extent of the array.

If a planar array lies in the XZ plane instead of the XY plane, then simply replace y_A and f_Y with z_A and f_Z , respectively, in (8.4-1), where spatial frequency f_Z is given by (1.2-45). And if a planar array lies in the YZ plane instead of the XY plane, then simply replace x_A and f_X with z_A and f_Z , respectively, in (8.4-1). As can be seen from (8.4-1), in order to derive the near-field beam pattern of a planar array, we must first specify a mathematical model for its complex frequency response.

Consider a planar array composed of an odd number $M \times N$ of identical, unevenly-spaced, complex-weighted, omnidirectional point-elements lying in the XY plane, where M and N are the total odd number of elements in the X and Y directions, respectively. The complex frequency response of this array is given by [see (8.1-20)]

$$A(f, x_A, y_A) = \mathcal{S}(f) \sum_{m=-M'}^{M'} \sum_{n=-N'}^{N'} c_{mn}(f) \delta(x_A - x_{mn}) \delta(y_A - y_{mn}), \quad (8.4-6)$$

where $\mathcal{S}(f)$ is the complex, element sensitivity function (see [Table 8.1-2](#) and [Appendix 6B](#)),

$$c_{mn}(f) = a_{mn}(f) \exp[+j\theta_{mn}(f)], \quad (8.4-7)$$

$$M' = (M-1)/2, \quad (8.4-8)$$

$$N' = (N-1)/2, \quad (8.4-9)$$

and the impulse functions $\delta(x_A - x_{mn})$ and $\delta(y_A - y_{mn})$ have units of inverse meters. Substituting (8.4-6) into (8.4-1) and making use of the sifting property of impulse functions yields the following expression for the near-field beam pattern:

$$\mathcal{D}(f, r, f_X, f_Y) = \mathcal{S}(f) \sum_{m=-M'}^{M'} \sum_{n=-N'}^{N'} c_{mn}(f) \exp\left[-j \frac{k}{2r} (x_{mn}^2 + y_{mn}^2)\right] \times \\ \exp\left[+j2\pi(f_X x_{mn} + f_Y y_{mn})\right]$$

$$(8.4-10)$$

If the elements are *equally spaced*, then $x_{mn} = md_X$ and $y_{mn} = nd_Y$ [see (8.1-22)

and (8.1-23)]. The units of $A(f, x_A, y_A)$ and $\mathcal{D}(f, r, f_X, f_Y)$ are summarized in [Table 8.4-1](#). Equation (8.4-10) is most accurate in the Fresnel region of the planar array where both the Fresnel angle criterion and the Fresnel range criterion are satisfied. It is less accurate in the near-field region outside the Fresnel region where $r < r_{\text{NF/FF}}$, but the Fresnel angle criterion is *not* satisfied. As was discussed in [Subsection 1.2.1](#), the Fresnel region is only a subset of the near-field.

Table 8.4-1 Units of the Complex Aperture Function $A(f, x_A, y_A)$ and Corresponding Near-Field Beam Pattern $\mathcal{D}(f, r, f_X, f_Y)$ for a Planar Array

Planar Array	$A(f, x_A, y_A)$	$\mathcal{D}(f, r, f_X, f_Y)$
active (transmit)	$((m^3/sec)/V)/m^2$	$(m^3/sec)/V$
passive (receive)	$(V/(m^2/sec))/m^2$	$V/(m^2/sec)$

8.4.1 Beam Steering and Array Focusing

We already know from planar aperture theory that in order to do beam steering and aperture focusing in the Fresnel region of a planar aperture, there must be a linear plus quadratic phase response across the surface of the aperture in both the X and Y directions (see [Subsection 3.5.1](#)). A set of phase weights that will produce a linear plus quadratic phase response across the surface of the planar array under discussion in both the X and Y directions is given by

$$\theta_{mn}(f) = -2\pi f'_X x_{mn} - 2\pi f'_Y y_{mn} + \frac{k}{2r'}(x_{mn}^2 + y_{mn}^2), \quad m = -M', \dots, 0, \dots, M' \\ n = -N', \dots, 0, \dots, N'$$

(8.4-11)

where

$$f'_X = u'/\lambda = \sin \theta' \cos \psi'/\lambda \quad (8.4-12)$$

$$f'_Y = v'/\lambda = \sin \theta' \sin \psi'/\lambda \quad (8.4-13)$$

and

$$k = 2\pi f/c = 2\pi/\lambda. \quad (8.4-14)$$

The parameter r' in (8.4-11) is the *focal range*. It is the near-field range from the

array where the far-field beam pattern of the array will be in focus. Compare (8.4-11) through (8.4-14) with (3.5-17) through (3.5-20).

If (8.4-7) and (8.4-11) are substituted into (8.4-10), then

$$\begin{aligned} \mathcal{D}(f, r, f_X, f_Y) = & \mathcal{S}(f) \sum_{m=-M'}^{M'} \sum_{n=-N'}^{N'} a_{mn}(f) \exp \left[-j \frac{k}{2} \left(\frac{1}{r} - \frac{1}{r'} \right) (x_{mn}^2 + y_{mn}^2) \right] \times \\ & \exp \left\{ +j2\pi \left[(f_X - f'_X)x_{mn} + (f_Y - f'_Y)y_{mn} \right] \right\}, \end{aligned} \quad (8.4-15)$$

and if (8.4-15) is evaluated at the near-field range $r = r'$, then it reduces to

$$\mathcal{D}(f, r', f_X, f_Y) = D(f, f_X - f'_X, f_Y - f'_Y), \quad (8.4-16)$$

where

$$D(f, f_X, f_Y) = \mathcal{S}(f) \sum_{m=-M'}^{M'} \sum_{n=-N'}^{N'} a_{mn}(f) \exp \left[+j2\pi(f_X x_{mn} + f_Y y_{mn}) \right] \quad (8.4-17)$$

is the far-field beam pattern of the array when it is only amplitude weighted. Equation (8.4-16) indicates that the far-field beam pattern $D(f, f_X, f_Y)$ of the amplitude weights $a_{mn}(f)$ is *in focus* at the near-field range $r = r'$ meters from the array, and has been *steered* in the direction $u = u'$ and $v = v'$ in direction-cosine space, which is equivalent to steering (tilting) the beam pattern to $\theta = \theta'$ and $\psi = \psi'$ [see (8.4-12) and (8.4-13)]. However, in the near-field region of the array outside the Fresnel region, a set of quadratic phase weights can only approximately focus the far-field beam pattern. Equal spacing of the elements is *not* required in order to do beam steering and array focusing.

As was discussed in [Section 8.2](#), a phase weight $\theta_{mn}(f)$ in radians is equivalent to a time delay τ'_{mn} in seconds, that is,

$$\theta_{mn}(f) \triangleq -2\pi f \tau'_{mn}, \quad (8.4-18)$$

or

$$\tau'_{mn} = -\theta_{mn}(f)/(2\pi f). \quad (8.4-19)$$

Substituting (8.4-11) through (8.4-14) into (8.4-19) yields

$$\tau'_{mn} = \frac{u'}{c} x_{mn} + \frac{v'}{c} y_{mn} - \frac{1}{2r'c} (x_{mn}^2 + y_{mn}^2), \quad m = -M', \dots, 0, \dots, M' \\ n = -N', \dots, 0, \dots, N'$$

$$(8.4-20)$$

where $c = f\lambda$. The phase weights given by (8.4-11) or, equivalently, the time delays given by (8.4-20) are implemented by using the beamforming procedure shown in Fig. 8.2-1.

8.5 FFT Beamforming for Planar Arrays

In this section we shall show how to implement complex weights in a planar array using the method of *FFT beamforming*. We shall also show how to compute the beam pattern of a planar array by using frequency-domain data already obtained from the method of FFT beamforming. The model that we shall use for the target is the same as that used in Subsection 1.2.2 and Section 7.2 – the target is modeled as an omnidirectional point-source located at $\mathbf{r}_s = (x_s, y_s, z_s)$ with arbitrary time dependence $s_0(t)$, where $s_0(t)$ is the source strength of the target in cubic meters per second (see Fig. 1.2-5). The model that we shall use for the fluid medium is the same as that used in Section 7.2 – the fluid medium is unbounded, viscous, and homogeneous (constant speed of sound).

The planar array in this section is being used in the passive mode, and is composed of an odd number $M \times N$ of identical, complex-weighted, omnidirectional point-elements lying in the XY plane, where M and N are the total odd number of elements in the X and Y directions, respectively. The elements are *equally spaced* in the X direction, and *equally spaced* in the Y direction. As a result, the x and y coordinates of the center of element (m, n) are given by $x_{mn} = x_m$ and $y_{mn} = y_n$ [see (8.1-22) and (8.1-23)]. Although the output electrical signals from the individual elements in the array are equal to the sum of the output electrical signals due to the target, ambient noise, and receiver noise; for example purposes, we shall only work with the output electrical signals due to the target. The procedure that we shall follow in this section is a two-dimensional generalization of the procedures used in Sections 7.2 and 7.3, and Subsection 7.3.1.

The output electrical signal in volts from element (m, n) in the array due to a sound-source (target) *before* complex weighting is given by

$$y'_{Trg}(t, x_m, y_n) = s(t - \tau_{mn}, x_m, y_n), \quad (8.5-1)$$

for $t \geq \tau_{mn}$, where

$$s(t, x_m, y_n) = F_f^{-1}\{S(f, x_m, y_n)\} = -\frac{1}{4\pi R_{mn}} F_f^{-1}\{S_0(f) \exp[-\alpha(f)R_{mn}] \mathcal{S}_R(f)\}, \quad (8.5-2)$$

$$R_{mn} = \sqrt{r_s^2 - 2r_s(u_s x_m + v_s y_n) + x_m^2 + y_n^2} \quad (8.5-3)$$

is the range in meters between the target and the center of element (m, n) ,

$$r_s = |\mathbf{r}_s| = \sqrt{x_s^2 + y_s^2 + z_s^2} \quad (8.5-4)$$

is the range to the target in meters as measured from the origin of the coordinate system (the center of the array) (see Fig. 1.2-5),

$$u_s = \sin \theta_s \cos \psi_s \quad (8.5-5)$$

and

$$v_s = \sin \theta_s \sin \psi_s \quad (8.5-6)$$

are dimensionless direction cosines with respect to the X and Y axes, respectively, associated with the target's location (see Fig. 1.2-6),

$$x_m = m d_x, \quad m = -M', \dots, 0, \dots, M', \quad (8.5-7)$$

and

$$y_n = n d_y, \quad n = -N', \dots, 0, \dots, N', \quad (8.5-8)$$

where

$$M' = (M - 1)/2 \quad (8.5-9)$$

and

$$N' = (N - 1)/2, \quad (8.5-10)$$

$S_0(f)$ is the complex frequency spectrum of the target's source strength in $(\text{m}^3/\text{sec})/\text{Hz}$, $\alpha(f)$ is the real, nonnegative, frequency-dependent, attenuation coefficient of the fluid medium in nepers (Np) per meter, $\mathcal{S}_R(f)$ is the complex, receiver sensitivity function with units of $\text{V}/(\text{m}^2/\text{sec})$ (see Table 8.1-2 and Appendix 6B), and

$$\tau_{mn} = R_{mn}/c \quad (8.5-11)$$

is the *one-way* time delay in seconds associated with the path length between the sound-source (target) and the center of element (m, n) . The spherical coordinates of the target's location (r_s, θ_s, ψ_s) are *unknown* a priori. Since element (m, n) is located at $\mathbf{r}_R = \mathbf{r}_{mn} = (x_m, y_n, 0)$, the range R_{mn} given by (8.5-3) was obtained by substituting $x_R = x_m$, $y_R = y_n$, $z_R = 0$, $x_s = r_s u_s$, and $y_s = r_s v_s$ into $R = |\mathbf{r}_R - \mathbf{r}_s| = \sqrt{(x_R - x_s)^2 + (y_R - y_s)^2 + (z_R - z_s)^2}$ and using (8.5-4).

The first step is to sample $y'_{Trgt}(t, x_m, y_n)$. If we sample $y'_{Trgt}(t, x_m, y_n)$ at a rate of f_s samples per second, then

$$y'_{Trgt}(t_l, x_m, y_n) = s(t_l - \tau_{mn}, x_m, y_n), \quad (8.5-12)$$

or

$$y'_{Trgt}(lT_S, md_X, nd_Y) = s(lT_S - \tau_{mn}, md_X, nd_Y), \quad (8.5-13)$$

where

$$t_l = lT_S, \quad l = 0, 1, \dots, L-1, \quad (8.5-14)$$

is the sampling time instant in seconds, $T_S = 1/f_S$ is the sampling period in seconds, and L is the total number of time samples taken. Note that

$$y'_{Trgt}(l, m, n) \equiv y'_{Trgt}(t_l, x_m, y_n) = y'_{Trgt}(lT_S, md_X, nd_Y). \quad (8.5-15)$$

By following the procedure shown in Fig. 7.3-1 for linear arrays, the second step is to compute the time-domain Fourier transform of $y'_{Trgt}(l, m, n)$. Using a modified version of the algorithm discussed in Appendix 7B for computing time-domain Fourier transforms yields

$$\hat{Y}'_{Trgt}(q, m, n) = T_S DFT_l \{ y'_{Trgt}(l, m, n) \}, \quad q = -L'', \dots, 0, \dots, L'', \quad (8.5-16)$$

or

$$\hat{Y}'_{Trgt}(q, m, n) = T_S \sum_{l=0}^{L-1} y'_{Trgt}(l, m, n) W_{L+Z}^{-ql}, \quad q = -L'', \dots, 0, \dots, L'', \quad (8.5-17)$$

where

$$\hat{Y}'_{Trgt}(q, m, n) \equiv \hat{Y}'_{Trgt}(qf_0, md_X, nd_Y) = \hat{Y}'_{Trgt}(f, x_m, y_n) \Big|_{f=qf_0} \quad (8.5-18)$$

is an estimate of the frequency spectrum of $y'_{Trgt}(t, x_m, y_n)$ at discrete frequencies $f = qf_0$,

$$W_{L+Z} = \exp \left(+j \frac{2\pi}{L+Z} \right), \quad (8.5-19)$$

$$f_0 = \frac{1}{T_0} = \frac{1}{(L+Z)T_S} = \frac{f_S}{L+Z} \quad (8.5-20)$$

is the frequency-domain DFT bin spacing [the fundamental frequency of $y'_{Trgt}(t, x_m, y_n)$] in hertz, T_0 is the fundamental period of $y'_{Trgt}(t, x_m, y_n)$ in seconds,

$$L'' = \begin{cases} (L+Z)/2, & L+Z \text{ even} \\ (L+Z-1)/2, & L+Z \text{ odd} \end{cases} \quad (8.5-21)$$

and Z is the total number of “zeros” used for “padding-with-zeros”. See Appendix 7B for an explanation of “padding-with-zeros”. Substituting (8.5-15) and (8.5-13) into (8.5-16) and using the time-shifting property of Fourier transforms yields

$$\begin{aligned}\hat{Y}'_{Trgt}(q, m, n) &= T_S DFT_l \left\{ s(lT_S - \tau_{mn}, md_X, nd_Y) \right\} \\ &= T_S DFT_l \left\{ s(l, m, n) \right\} \exp(-j2\pi q f_0 \tau_{mn}), \quad q = -L'', \dots, 0, \dots, L'',\end{aligned}\quad (8.5-22)$$

or

$$\hat{Y}'_{Trgt}(q, m, n) = \hat{S}(q, m, n) \exp(-j2\pi q f_0 \tau_{mn}), \quad (8.5-23)$$

where

$$\hat{S}(q, m, n) = T_S DFT_l \left\{ s(l, m, n) \right\}, \quad q = -L'', \dots, 0, \dots, L'', \quad (8.5-24)$$

is an estimate of the theoretical frequency spectrum [see (8.5-2)]

$$S(f, x_m, y_n) = -\frac{1}{4\pi R_{mn}} S_0(f) \exp[-\alpha(f) R_{mn}] \mathcal{S}_R(f) \quad (8.5-25)$$

at discrete frequencies $f = qf_0$, and

$$s(l, m, n) \equiv s(t_l, x_m, y_n) = s(lT_S, md_X, nd_Y). \quad (8.5-26)$$

As can be seen from (8.5-25), $S(f, x_m, y_n)$ is related to the complex frequency spectrum of the target's source strength $S_0(f)$.

The third step is to multiply $\hat{Y}'_{Trgt}(q, m, n)$ by the complex weight

$$c_{mn}(qf_0) = a_{mn} \exp[+j\theta_{mn}(qf_0)] = a_{mn} \exp(-j2\pi q f_0 \tau'_{mn}). \quad (8.5-27)$$

Doing so yields

$$\hat{Y}_{Trgt}(q, m, n) = \hat{Y}'_{Trgt}(q, m, n) c_{mn}(qf_0), \quad (8.5-28)$$

and by substituting (8.5-23) and (8.5-27) into (8.5-28), we obtain

$$\hat{Y}_{Trgt}(q, m, n) = a_{mn} \hat{S}(q, m, n) \exp[-j2\pi q f_0 (\tau_{mn} + \tau'_{mn})]. \quad (8.5-29)$$

The fourth and final step is to compute the inverse Fourier transform of $\hat{Y}_{Trgt}(q, m, n)$. The inverse Fourier transform of $\hat{Y}_{Trgt}(q, m, n)$ is computed as follows:

$$\hat{y}_{Trgt}(l, m, n) = \frac{1}{T_S} IDFT_q \left\{ \hat{Y}_{Trgt}(q, m, n) \right\}, \quad l = 0, 1, \dots, L + Z - 1, \quad (8.5-30)$$

or

$$\hat{y}_{Trgt}(l, m, n) = \frac{1}{T_s} \frac{1}{L+Z} \sum_{q=-L''}^{L''} \hat{Y}_{Trgt}(q, m, n) W_{L+Z}^{ql}, \quad l = 0, 1, \dots, L+Z-1, \quad (8.5-31)$$

where IDFT is the abbreviation for inverse discrete Fourier transform. Substituting (8.5-29) into (8.5-30) yields

$$\begin{aligned} \hat{y}_{Trgt}(l, m, n) &= a_{mn} \frac{1}{T_s} IDFT_q \left\{ \hat{S}(q, m, n) \exp[-j2\pi q f_0 (\tau_{mn} + \tau'_{mn})] \right\}, \\ l &= 0, 1, \dots, L+Z-1, \end{aligned} \quad (8.5-32)$$

and by using the time-shifting property of Fourier transforms, we obtain

$$\hat{y}_{Trgt}(l, m, n) = a_{mn} \hat{s}(l T_s - [\tau_{mn} + \tau'_{mn}], m, n), \quad l = 0, 1, \dots, L+Z-1, \quad (8.5-33)$$

which is an estimate of time samples of the output electrical signal $y_{Trgt}(t, x_m, y_n)$ from element (m, n) in the array due to the target *after* complex weighting, where

$$\hat{s}(l, m, n) = \frac{1}{T_s} IDFT_q \left\{ \hat{S}(q, m, n) \right\} \quad (8.5-34)$$

is an *estimate* of time samples of $s(t, x_m, y_n)$ given by (8.5-2) because $\hat{Y}_{Trgt}(q, m, n)$ was obtained by multiplying the *estimate* $\hat{Y}'_{Trgt}(q, m, n)$ by the complex weight $c_{mn}(q f_0)$ [see (8.5-28)].

In order to compute the beam pattern of the planar array, compute the *two-dimensional spatial* DFT of the frequency-domain data $\hat{Y}_{Trgt}(q, m, n)$ already obtained from the method of FFT beamforming. As discussed in [Section 8.3](#), a two-dimensional spatial DFT can be computed as a sequence of two, one-dimensional spatial DFTs. First compute the spatial DFT of $\hat{Y}_{Trgt}(q, m, n)$ in the X direction as follows:

$$\hat{Y}_{Trgt}(q, r, n) = DFT_m \left\{ \hat{Y}_{Trgt}(q, m, n) \right\}, \quad r = -M'', \dots, 0, \dots, M'', \quad (8.5-35)$$

or (see [Section 8.3](#))

$$\hat{Y}_{Trgt}(q, r, n) = \sum_{m=-M'}^{M'} \hat{Y}_{Trgt}(q, m, n) W_{M+Z_X}^{rm}, \quad r = -M'', \dots, 0, \dots, M'', \quad (8.5-36)$$

where W_{M+Z_X} is given by (8.3-12), M'' is given by (8.3-9), the DFT bin number r corresponds to discrete spatial frequency $f_X = r\Delta f_X$, where Δf_X is the spatial-frequency spacing in the X direction (with units of cycles per meter) given by (8.3-7), and Z_X is the total number of “zeros” used for “padding-with-zeros” in the X direction. The value of direction cosine u at DFT bin r is u_r given by (8.3-23).

Next, compute the spatial DFT of $\hat{Y}_{Trgt}(q, r, n)$ in the Y direction as follows:

$$\hat{Y}_{Trgt}(q, r, s) = DFT_n \left\{ \hat{Y}_{Trgt}(q, r, n) \right\}, \quad s = -N'', \dots, 0, \dots, N'', \quad (8.5-37)$$

or (see [Section 8.3](#))

$$\hat{Y}_{Trgt}(q, r, s) = \sum_{n=-N'}^{N'} \hat{Y}_{Trgt}(q, r, n) W_{N+Z_Y}^{sn}, \quad s = -N'', \dots, 0, \dots, N'', \quad (8.5-38)$$

where W_{N+Z_Y} is given by (8.3-13), N'' is given by (8.3-10), the DFT bin number s corresponds to discrete spatial frequency $f_Y = s\Delta f_Y$, where Δf_Y is the spatial-frequency spacing in the Y direction (with units of cycles per meter) given by (8.3-8), and Z_Y is the total number of “zeros” used for “padding-with-zeros” in the Y direction. The value of direction cosine v at DFT bin s is v_s given by (8.3-26). The function $\hat{Y}_{Trgt}(q, r, s)$ is an estimate of the frequency-and-angular spectrum of $y_{Trgt}(t, x_m, y_n)$ at discrete frequencies $f = qf_0$, and discrete spatial frequencies $f_X = r\Delta f_X$ and $f_Y = s\Delta f_Y$, or equivalently, direction cosine values u_r and v_s . The function $y_{Trgt}(t, x_m, y_n)$ is the output electrical signal (in volts) from element (m, n) in the array due to the target *after* complex weighting. Next we shall show that $\hat{Y}_{Trgt}(q, r, s)$ is related to the beam pattern of the planar array.

For example, if the sound-source (target) is in the far-field region of the array, then set $R_{mn} = r_s$ in (8.5-25) so that $S(f, x_m, y_n) \approx S(f)$ where

$$S(f) = -\frac{1}{4\pi r_s} S_0(f) \exp[-\alpha(f)r_s] \mathcal{S}_R(f). \quad (8.5-39)$$

Also, in order to obtain a good approximation of the time delay τ_{mn} , start by substituting (7.2-8) and $\mathbf{r}_R = md_x \hat{x} + nd_y \hat{y}$ into (7.2-37). Doing so yields

$$R_{mn} \approx r_s - u_s m d_x - v_s n d_y, \quad (8.5-40)$$

and by substituting (8.5-40) into (8.5-11), we obtain

$$\tau_{mn} \approx \tau_s - \frac{u_s}{c} md_x - \frac{v_s}{c} nd_y , \quad (8.5-41)$$

where

$$\tau_s = r_s/c \quad (8.5-42)$$

is the *one-way* time delay in seconds associated with the path length between the sound-source (target) and the center of the array. The time delay τ_s is also *unknown* a priori because the range r_s is unknown a priori. Based on the model for τ_{mn} given by (8.5-41), ignoring τ_s and since u_s and v_s are unknown a priori (see [Section 8.2](#)),

$$\tau'_{mn} = \frac{u'}{c} md_x + \frac{v'}{c} nd_y . \quad (8.5-43)$$

Adding (8.5-41) and (8.5-43) yields

$$\tau_{mn} + \tau'_{mn} = \tau_s + \frac{1}{c} (u' - u_s) md_x + \frac{1}{c} (v' - v_s) nd_y . \quad (8.5-44)$$

Substituting (8.5-44) into (8.5-29), and replacing $\hat{S}(q, m, n)$ with $\hat{S}(q)$ yields

$$\begin{aligned} \hat{Y}_{Trgt}(q, m, n) &= \hat{S}(q) \exp(-j2\pi q f_0 \tau_s) \times \\ &a_{mn} \exp \left\{ -j2\pi q f_0 \left[\frac{(u' - u_s)}{c} md_x + \frac{(v' - v_s)}{c} nd_y \right] \right\}, \end{aligned} \quad (8.5-45)$$

where $\hat{S}(q)$ is an estimate of the theoretical frequency spectrum $S(f)$ given by (8.5-39) at discrete frequencies $f = q f_0$. As can be seen from (8.5-39), $S(f)$ is related to the complex frequency spectrum of the target's source strength $S_0(f)$. Note that when $u' \neq u_s$ and $v' \neq v_s$, the *phase* of $\hat{Y}_{Trgt}(q, m, n)$ given by (8.5-45) is *different* at each element (m, n) . As a result, the output electrical signals from each element in the array will be *out-of-phase*.

If the far-field beam pattern of the array is steered in the direction of the acoustic field incident upon the array (in this case, $\theta' = \theta_s$ and $\psi' = \psi_s$ so that $u' = u_s$ and $v' = v_s$), then (8.5-45) reduces to

$$\hat{Y}_{Trgt}(q, m, n) = \hat{S}(q) \exp(-j2\pi q f_0 \tau_s) a_{mn} . \quad (8.5-46)$$

The *phase* of $\hat{Y}_{Trgt}(q, m, n)$ given by (8.5-46) is now the *same* at each element (m, n) . Therefore, the output electrical signals from each element in the array will be *in-phase* and, as a result, the array gain will be *maximized*. Substituting (8.5-46) into (8.5-36) yields

$$\hat{Y}_{Trgt}(q, r, n) = \hat{S}(q) \exp(-j2\pi q f_0 \tau_s) \sum_{m=-M'}^{M'} a_{mn} W_{M+Z_X}^{rm}, \quad r = -M'', \dots, 0, \dots, M'', \quad (8.5-47)$$

and substituting (8.5-47) into (8.5-38) yields

$$\hat{Y}_{Trgt}(q, r, s) = \hat{S}(q) \exp(-j2\pi q f_0 \tau_s) \sum_{m=-M'}^{M'} \sum_{n=-N'}^{N'} a_{mn} W_{M+Z_X}^{rm} W_{N+Z_Y}^{sn}, \quad (8.5-48)$$

$$r = -M'', \dots, 0, \dots, M'', \quad s = -N'', \dots, 0, \dots, N''.$$

The double summation in (8.5-48) is the *array factor* for the set of amplitude weights a_{mn} . The array factor is directly proportional to the far-field beam pattern of the array. At broadside, that is, at $r = 0$ and $s = 0$, (8.5-48) reduces to

$$\hat{Y}_{Trgt}(q, 0, 0) = \hat{S}(q) \exp(-j2\pi q f_0 \tau_s) \sum_{m=-M'}^{M'} \sum_{n=-N'}^{N'} a_{mn}. \quad (8.5-49)$$

When $u' \neq u_s$ and $v' \neq v_s$, substituting (8.5-45) into (8.5-36) yields

$$\hat{Y}_{Trgt}(q, r, n) = \hat{S}(q) \exp(-j2\pi q f_0 \tau_s) \exp\left[-j2\pi q f_0 \frac{(v' - v_s)}{c} n d_Y\right] \times$$

$$\sum_{m=-M'}^{M'} a_{mn} \exp\left[-j2\pi q f_0 \frac{(u' - u_s)}{c} m d_X\right] W_{M+Z_X}^{rm},$$

$$r = -M'', \dots, 0, \dots, M'', \quad (8.5-50)$$

and substituting (8.5-50) into (8.5-38) yields

$$\hat{Y}_{Trgt}(q, r, s) = \hat{S}(q) \exp(-j2\pi q f_0 \tau_s) \times$$

$$\sum_{m=-M'}^{M'} \sum_{n=-N'}^{N'} a_{mn} \exp\left\{-j2\pi q f_0 \left[\frac{(u' - u_s)}{c} m d_X + \frac{(v' - v_s)}{c} n d_Y\right]\right\} W_{M+Z_X}^{rm} W_{N+Z_Y}^{sn},$$

$$r = -M'', \dots, 0, \dots, M'', \quad s = -N'', \dots, 0, \dots, N''. \quad (8.5-51)$$

The double summation in (8.5-51) is the array factor for the set of amplitude weights a_{mn} steered in the direction $u = u' - u_s$ and $v = v' - v_s$ in direction-cosine space.

In order to prove the above statement, we need to find the values of DFT bins r and s , or equivalently, direction cosines $u = u_r$ and $v = v_s$, so that (8.5-51) reduces to (8.5-49). Start by substituting (8.3-12) and (8.3-13) into (8.5-51). Doing so yields

$$\begin{aligned} \hat{Y}_{Trgt}(q, r, s) &= \hat{S}(q) \exp(-j2\pi q f_0 \tau_s) \times \\ &\sum_{m=-M'}^{M'} \sum_{n=-N'}^{N'} a_{mn} \exp \left\{ -j2\pi \left[q f_0 \frac{(u' - u_s)}{c} d_x - \frac{r}{M + Z_x} \right] m \right\} \times \\ &\exp \left\{ -j2\pi \left[q f_0 \frac{(v' - v_s)}{c} d_y - \frac{s}{N + Z_y} \right] n \right\}. \end{aligned} \quad (8.5-52)$$

As can be seen from (8.5-52), the values of r and s that will reduce (8.5-52) to (8.5-49) are

$$r = r' = (M + Z_x) q f_0 \frac{(u' - u_s)}{c} d_x \quad (8.5-53)$$

and

$$s = s' = (N + Z_y) q f_0 \frac{(v' - v_s)}{c} d_y \quad (8.5-54)$$

since these values of r and s will cause the exponents inside the double summation to be equal to 0. Although the parameter values on the right-hand sides of (8.5-53) and (8.5-54) are such that r' and s' are not integers in general, for example purposes, we shall assume they are. Therefore, substituting (8.5-53) and (8.5-54) into (8.3-23) and (8.3-26), respectively, and since

$$c = f\lambda = q f_0 \lambda, \quad (8.5-55)$$

then

$$u_{r'} = u' - u_s \quad (8.5-56)$$

and

$$v_{s'} = v' - v_s. \quad (8.5-57)$$

In other words, when $u' \neq u_s$ and $v' \neq v_s$, the value of the array factor at broadside will be located at $u = u' - u_s$ and $v = v' - v_s$ in direction-cosine space, that is, the array factor will be steered to $u = u' - u_s$ and $v = v' - v_s$.

If no beam steering is done, that is, if $u' = 0$ and $v' = 0$, then $u_{r'} = -u_s$ and

$v_{s'} = -v_S$, or $-u_{r'} = u_S$ and $-v_{s'} = v_S$. Substituting

$$u = -u_{r'} \quad (8.5-58)$$

and

$$v = -v_{s'} \quad (8.5-59)$$

into (3.2-9) and (3.2-10) yields

$$\theta_S = \sin^{-1} \sqrt{u_{r'}^2 + v_{s'}^2}, \quad \sqrt{u_{r'}^2 + v_{s'}^2} \leq 1 \quad (8.5-60)$$

and

$$\psi_S = \tan^{-1}(v_{s'}/u_{r'}), \quad (8.5-61)$$

which are the angles in the direction of the acoustic field incident upon the array. In order to obtain the correct value for the azimuthal (bearing) angle ψ_S , one must take into account the signs (quadrant) of the $(-u_{r'}, -v_{s'}) = (u_S, v_S)$ coordinates (see [Table 3.2-1](#)).

Problems

Section 8.1

- 8-1 Consider a planar array composed of an odd number $M \times N$ of identical, equally-spaced, complex-weighted elements lying in the XY plane, where M and N are the total odd number of elements in the X and Y directions, respectively. If the complex weight $c_{mn}(f)$ satisfies the conjugate symmetry property $c_{-m-n}(f) = c_{mn}^*(f)$, then what does (8.1-14) reduce to?
- 8-2 Consider a planar array composed of an odd number $M \times N$ of identical, equally-spaced, complex-weighted elements lying in the XY plane, where M and N are the total odd number of elements in the X and Y directions, respectively. The complex weights are separable, rectangular amplitude weights are used in both the X and Y directions, and *no* phase weighting is done.
- (a) If the elements are omnidirectional point-elements, then find the unnormalized, far-field beam pattern of this array as a function of frequency f and direction cosines u and v .
 - (b) If the elements are rectangular pistons whose size is small compared to a wavelength so that (8.1-27) and (8.1-28) are satisfied, then find the unnormalized, far-field beam pattern of this array as a function of

frequency f and direction cosines u and v .

- (c) If the elements are circular pistons whose circumference is small compared to a wavelength so that (8.1-34) is satisfied, then find the unnormalized, far-field beam pattern of this array as a function of frequency f and direction cosines u and v .
- 8-3 A side-looking sonar (SLS) is modeled as a planar array composed of an odd number $M \times N$ of identical, equally-spaced, complex-weighted, omnidirectional point-elements lying in the YZ plane (see Fig. 5.1-1), where M and N are the total odd number of elements in the Y and Z directions, respectively, and d_y and d_z are the interelement spacings in meters.
- (a) If the complex weights are separable, rectangular amplitude weights are used in both the Y and Z directions, and *no* phase weighting is done, then find the unnormalized, far-field beam pattern of this array as a function of frequency f and direction cosines v and w .
- Using the specifications of the SLS from Example 5.7-1, if the lengths of the array in the Y and Z directions are $L_{AY} = 0.1$ m and $L_{AZ} = 2.5$ m, respectively, the operating frequency is 30 kHz, half-wavelength interelement spacing is used in both the Y and Z directions, and $c = 1500$ m/sec, then
- (b) how many elements are there in the Y direction?
 - (c) how many elements are there in the Z direction?
 - (d) what is the maximum possible value of array gain?
- 8-4 If the length of the sides of the equilateral triangle formed by a triplet circular array is d meters, then
- (a) find the relationship between the radius a of the triplet and d .
 - (b) If $ka = \pi/3$ as in Example 8.1-7, then find the value of the ratio d/λ .
 - (c) If $ka = \pi/3$ and $c = 1500$ m/sec, then find the radius a of the triplet and the interelement spacing d for the following frequencies: $f = 100$ Hz, 500 Hz, and 1 kHz.
- 8-5 Consider a linear array composed of an odd number M of identical, unevenly-spaced, complex-weighted elements lying in the XY plane. Find the unnormalized, far-field beam pattern of this array if

- (a) the linear array is lying along the X axis.
- (b) the linear array is lying along the Y axis.

- 8-6 Consider a linear array composed of an odd number M of identical, unevenly-spaced, complex-weighted elements lying in the XZ plane. Find the unnormalized, far-field beam pattern of this array if
- (a) the linear array is lying along the Z axis.
 - (b) the elements are equally-spaced rectangular pistons, rectangular amplitude weights are used, *no* phase weighting is done, and the linear array is lying along the Z axis.

Section 8.2

- 8-7 (a) Repeat Problem 8-3 (a) using rectangular amplitude weights *and* linear phase weights in both the Y and Z directions.
- (b) Find the equations for the phase weights and equivalent time delays that will steer the far-field beam pattern of this array to $\theta' = 90^\circ$ and $\psi' = 37.71^\circ$ (see [Example 5.7-1](#) and [Table 5.7-2](#)).
- 8-8 Find the equations for the phase weights and equivalent time delays that are required in order to steer the far-field beam pattern of the tesseral quadrupole discussed in [Example 8.1-4](#).
- 8-9 Find the equations for the phase weights and equivalent time delays that will steer the far-field beam pattern of a planar array of concentric circular arrays of identical, equally-spaced, complex-weighted, omnidirectional point-elements lying in the XY plane.
- 8-10 Find the equations for the phase weights and equivalent time delays that are required in order to steer the mainlobe of the far-field beam pattern of the linear array in the XY plane discussed in [Example 8.1-8](#) for the case of identical, unevenly-spaced, omnidirectional point-elements.

Section 8.3

- 8-11 A planar array of 505 identical, equally-spaced, complex-weighted, omnidirectional point-elements is lying in the XY plane, where the total number of elements in the X and Y directions are 101 and 5, respectively. Half-wavelength interelement spacing is used in both the X and Y directions. A two-dimensional, spatial DFT is used to compute the far-field beam pattern of the array.

- (a) What are the direction-cosine bin spacings δu and δv if “padding-with-zeros” is not done?
- (b) Solve for the number of “zeros” that are required in order to obtain direction-cosine bin spacings $\delta u = 0.01$ and $\delta v = 0.01$.
- (c) Using your answers from Part (b), find the values of direction cosines u and v at DFT bins $r = -50$ and $s = 75$.
- (d) Using your answers from Part (c), find the values of the vertical angle θ and the azimuthal (bearing) angle ψ at DFT bins $r = -50$ and $s = 75$.

Appendix 8A Two-Dimensional Spatial FIR Filters

The Product Theorem for a planar array composed of an odd number of identical elements is given by [see (8.1-12)]

$$D(f, f_X, f_Y) = E(f, f_X, f_Y)S(f, f_X, f_Y), \quad (8A-1)$$

where $D(f, f_X, f_Y)$ is the far-field beam pattern of the array, $E(f, f_X, f_Y)$ is the far-field beam pattern of *one* of the identical elements in the array, and

$$S(f, f_X, f_Y) = \sum_{m=-M'}^{M'} \sum_{n=-N'}^{N'} c_{mn}(f) \exp\left[+j2\pi(f_X x_{mn} + f_Y y_{mn})\right] \quad (8A-2)$$

is the dimensionless array factor [see (8.1-14)]. Taking the inverse two-dimensional spatial Fourier transform of the Product Theorem given by (8A-1) yields

$$A(f, x_A, y_A) = e(f, x_A, y_A) \underset{x_A, y_A}{\ast\ast} s(f, x_A, y_A), \quad (8A-3)$$

where

$$s(f, x_A, y_A) = F_{f_X}^{-1} F_{f_Y}^{-1} \{ S(f, f_X, f_Y) \} = \sum_{m=-M'}^{M'} \sum_{n=-N'}^{N'} c_{mn}(f) \delta(x_A - x_{mn}) \delta(y_A - y_{mn}) \quad (8A-4)$$

since

$$\begin{aligned} F_{f_X}^{-1} F_{f_Y}^{-1} \left\{ \exp\left[+j2\pi(f_X x_{mn} + f_Y y_{mn})\right] \right\} &= F_{f_X}^{-1} \left\{ \exp(+j2\pi f_X x_{mn}) \right\} F_{f_Y}^{-1} \left\{ \exp(+j2\pi f_Y y_{mn}) \right\} \\ &= \delta(x_A - x_{mn}) \delta(y_A - y_{mn}). \end{aligned} \quad (8A-5)$$

If the elements are omnidirectional point-elements, then the element function $e(f, x_A, y_A)$ is given by [see (8.1-16)]

$$e(f, x_A, y_A) = \mathcal{S}(f) \delta(x_A, y_A) = \mathcal{S}(f) \delta(x_A) \delta(y_A), \quad (8A-6)$$

where $\mathcal{S}(f)$ is the element sensitivity function. If we set $\mathcal{S}(f) = 1(m^3/\text{sec})/V$ or $\mathcal{S}(f) = 1V/(m^2/\text{sec})$, then (8A-6) reduces to

$$e(f, x_A, y_A) = \delta(x_A) \delta(y_A). \quad (8A-7)$$

Substituting the “input signal” given by (8A-7) into (8A-3) yields the “output signal”

$$A(f, x_A, y_A) = \delta(x_A) \delta(y_A) * s(f, x_A, y_A) = s(f, x_A, y_A), \quad (8A-8)$$

where $s(f, x_A, y_A)$ given by (8A-4) can be thought of as the two-dimensional, spatial impulse response of the array at frequency f hertz. Since (8A-4) is in the form of the impulse response of a two-dimensional, finite impulse response (FIR) digital filter, a planar array composed of an odd number of identical, complex-weighted elements can be thought of as a two-dimensional, spatial FIR filter.

Appendix 8B Normalization Factor for the Array Factor

The general expression for the array factor $S(f, f_X, f_Y)$ for M and N odd is given by [see (8.1-14)]

$$S(f, f_X, f_Y) = \sum_{m=-M'}^{M'} \sum_{n=-N'}^{N'} c_{mn}(f) \exp\left[+j2\pi(f_X x_{mn} + f_Y y_{mn})\right]. \quad (8B-1)$$

Computing the magnitude of $S(f, f_X, f_Y)$ yields

$$\begin{aligned} |S(f, f_X, f_Y)| &= \left| \sum_{m=-M'}^{M'} \sum_{n=-N'}^{N'} c_{mn}(f) \exp\left[+j2\pi(f_X x_{mn} + f_Y y_{mn})\right] \right| \\ &\leq \sum_{m=-M'}^{M'} \sum_{n=-N'}^{N'} \left| c_{mn}(f) \exp\left[+j2\pi(f_X x_{mn} + f_Y y_{mn})\right] \right| \quad (8B-2) \\ &\leq \sum_{m=-M'}^{M'} \sum_{n=-N'}^{N'} \left| c_{mn}(f) \right| \left| \exp\left[+j2\pi(f_X x_{mn} + f_Y y_{mn})\right] \right|, \end{aligned}$$